N-1796

July 1989

NCEL

Technical Note

By T.S. Huang and J.W. Leonard

Sponsored By Naval Facilities Engineering Command

LATERAL STABILITY OF A FLEXIBLE SUBMARINE HOSELINE

ABSTRACT The lateral stability of a submarine hoseline in a slowly varying current is investigated. If the current force overcomes the sea bottom resistance, the hose segment is assumed to slide on the sea bottom without twisting. The stability is evaluated in terms of lateral deflections, hose tensions, and anchor loads. The behavior of a hoseline in a variable current is simulated based on nonlinear cable-like response to lift and Morison-type drag forces. Principles and the numerical algorithm of the simulation model are briefly summarized. A parametric analysis is conducted to study the influence on the hose response of the physical parameters considered in the simulation model. The results indicate that, for a practical hoseline, the most critical parameters are: the segment length-to-span ratio, the axial rigidity of the hose, the hose size, and the current velocity. The sea bottom resistance is negligible from a design point of view. Keywords: Underwater pipelines; (ET)

NAVAL CIVIL ENGINEERING LABORATORY PORT HUENEME CALIFORNIA 93043

METRIC CONVERSION FACTORS

Approximate Conversions to Metric Measures

Symbol	When You Know	Multiply by	To Find	Symbol
		LENGTH		
in	inches	*2.5	centimeters	cm
ft	feet	30	centimeters	cm
yd	yards	0.9	meters	m
mi	miles	1.6	kilometers	km
		AREA		
in^2	square inches	6.5	square centimeters	cm^2
ft^2	square feet	0.09	square meters	m^2
yd^2	square yards	0.8	square meters	m^2
mi^2	square miles	2.6	square kilometers	km^2
	acres	0.4	hectares	ha
		MASS (weight)		
oz	ounces	28	grams	g
lb	pounds	0.45	kilograms	kg
	short tons (2,000 lb)	0.9	tonnes	t
		VOLUME		
tsp	teaspoons	5	milliliters	ml
Tbsp	tablespoons	15	milliliters	ml
fl oz	fluid ounces	30	milliliters	ml
c	cups	0.24	liters	l
pt	pints	0.47	liters	l
qt	quarts	0.95	liters	l
gal	gallons	3.8	liters	l
ft^3	cubic feet	0.03	cubic meters	m^3
yd^3	cubic yards	0.76	cubic meters	m^3
		TEMPERATURE (exact)		
°F	Fahrenheit temperature	5/9 (after subtracting 32)	Celsius temperature	°C

*1 in = 2.54 (exactly). For other exact conversions and more detailed tables, see NBS Misc. Publ. 286, Units of Weights and Measures, Price $2.25, SD Catalog No. C13.10:286.

Approximate Conversions from Metric Measures

Symbol	When You Know	Multiply by	To Find	Symbol
		LENGTH		
mm	millimeters	0.04	inches	in
cm	centimeters	0.4	inches	in
m	meters	3.3	feet	ft
m	meters	1.1	yards	yd
km	kilometers	0.6	miles	mi
		AREA		
cm^2	square centimeters	0.16	square inches	in^2
m^2	square meters	1.2	square yards	yd^2
km^2	square kilometers	0.4	square miles	mi^2
ha	hectares (10,000 m^2)	2.5	acres	
		MASS (weight)		
g	grams	0.035	ounces	oz
kg	kilograms	2.2	pounds	lb
t	tonnes (1,000 kg)	1.1	short tons	
		VOLUME		
ml	milliliters	0.03	fluid ounces	fl oz
l	liters	2.1	pints	pt
l	liters	1.06	quarts	qt
l	liters	0.26	gallons	gal
m^3	cubic meters	35	cubic feet	ft^3
m^3	cubic meters	1.3	cubic yards	yd^3
		TEMPERATURE (exact)		
°C	Celsius temperature	9/5 (then add 32)	Fahrenheit temperature	°F

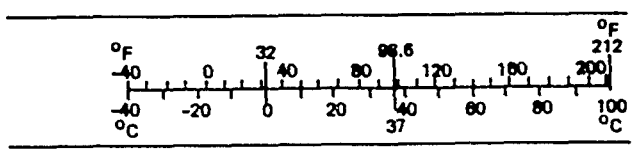

Unclassified

SECURITY CLASSIFICATION OF THIS PAGE *(When Data Entered)*

REPORT DOCUMENTATION PAGE		READ INSTRUCTIONS BEFORE COMPLETING FORM
1 REPORT NUMBER TN-1796	2. GOVT ACCESSION NO. DN669044	3. RECIPIENT'S CATALOG NUMBER
4. TITLE *(and Subtitle)* LATERAL STABILITY OF A FLEXIBLE SUBMARINE HOSELINE		5. TYPE OF REPORT & PERIOD COVERED Final; Oct 1986 - Sep 1987 6 PERFORMING ORG. REPORT NUMBER
7. AUTHOR(s) T.S. Huang, NCEL, and J.W. Leonard, Oregon State Univ.		8. CONTRACT OR GRANT NUMBER(s)
9. PERFORMING ORGANIZATION NAME AND ADDRESS NAVAL CIVIL ENGINEERING LABORATORY Port Hueneme, California 93043-5003		10 PROGRAM ELEMENT, PROJECT, TASK AREA & WORK UNIT NUMBERS RM-33-U62-30-N14B
11. CONTROLLING OFFICE NAME AND ADDRESS Office of Naval Technology Arlington, Virginia 22217-5000		12. REPORT DATE July 1989 13 NUMBER OF PAGES 64
14 MONITORING AGENCY NAME & ADDRESS*(if different from Controlling Office)*		15. SECURITY CLASS. *(of this report)* Unclassified 15a. DECLASSIFICATION/DOWNGRADING SCHEDULE

16. DISTRIBUTION STATEMENT *(of this Report)*

Approved for public release; distribution is unlimited.

DISTRIBUTION STATEMENT *(of the abstract entered in Block 20, if different from Report)*

18. SUPPLEMENTARY NOTES

19 KEY WORDS *(Continue on reverse side if necessary and identify by block number)*

Hoseline, flexible, submarine, lateral currents, tension, anchor load, deflection, simulation

20 ABSTRACT *(Continue on reverse side if necessary and identify by block number)*

The lateral stability of a submarine hoseline in a slowly varying current is investigated. If the current force overcomes the sea bottom resistance, the hose segment is assumed to slide on the sea bottom without twisting. The stability is evaluated in terms of lateral deflections, hose tensions, and anchor loads. The behavior of a hoseline in a variable current is simulated based nonlinear cable-like response to lift and Morison-type drag forces. Principles and the numerical algorithm of the simulation model

Continued

DD FORM 1 JAN 73 1473 EDITION OF 1 NOV 55 IS OBSOLETE

Unclassified

SECURITY CLASSIFICATION OF THIS PAGE *(When Data Entered)*

20. Continued

are briefly summarized. A parametric analysis is conducted to study the influence on the hose response of the physical parameters considered in the simulating model. The results indicate that, for a practical hoseline, the most critical parameters are: the segment length-to-span ratio, the axial rigidity of the hose, the hose size, and the current velocity. The sea bottom resistance is negligible from a design point of view.

Library Card

Naval Civil Engineering Laboratory
LATERAL STABILITY OF A FLEXIBLE SUBMARINE HOSELINE
(Final), by T.S. Huang and J.W. Leonard
TN-1796 64 pp illus July 1989 Unclassified

1. Hoseline 2. Flexible I. RM-33-U62-30-N14B

The lateral stability of a submarine hoseline in a slowly varying current is investigated. If the current force overcomes the sea bottom resistance, the hose segment is assumed to slide on the sea bottom without twisting. The stability is evaluated in terms of lateral deflections, hose tensions, and anchor loads. The behavior of a hoseline in a variable current is simulated based nonlinear cable-like response to lift and Morison-type drag forces. Principles and the numerical algorithm of the simulation model are briefly summarized. A parametric analysis is conducted to study the influence on the hose response of the physical parameters considered in the simulating model. The results indicate that, for a practical hoseline, the most critical parameters are: the segment length-to-span ratio, the axial rigidity of the hose, the hose size, and the current velocity. The sea bottom resistance is negligible from a design point of view.

CONTENTS

INTRODUCTION

Objective

The objective of this study was to determine analytically the lateral stability of the Navy's flexible submarine hoselines in a slowly varying current. This goal was achieved through the development of three easy to use design tools: a numerical simulation model, design charts, and a parametric model.

Scope

This effort analyzed the lateral stability of a flexible submarine hoseline in varying currents. The analysis was limited to a long hose of little flexural and torsional stiffness. Further, only the behavior of a taut hose segment was studied. The response of a slack hose segment, which has zero axial tension, was not included. Theories for simulating the behaviors of a submarine hoseline in currents were derived. Design tools were developed to provide the required stability for engineering applications.

This report presents the development of the hoseline simulation model. Pertinent theories used in the derivation of the model are briefly described. The numerical solution techniques incorporated in the computer code are included in Appendix A. The procedures and major findings obtained from the parametric analysis are also discussed. Results of the analysis are presented in graphs to show the influence of each governing parameter. Design charts and parametric models for typical Navy hoses are presented followed by a guideline for using these results for design.

Background

Large volumes of fuels are consumed daily by amphibious forces when engaged on a battle field. Liquid cargo of the required volume can be transferred only by tankers, which may be moored several miles from shore. The cargo is discharged through conduits to the beachhead. Time is a critical factor; it dominates system design in addition to functional reliability. Thus, the most effective system is the one that is transported easily and rapidly, requires the least resources for installation and operation, and is largely universal. The Naval Civil Engineering Laboratory (NCEL) is currently developing a flexible high-strength conduit to maximize the effectiveness of the Navy's liquid cargo handling system. The conduit, which is highly collapsible and allows a very small bending radius, could be compactly spooled on hose reels for easy storage and transportation.

Among the engineering considerations, the most important factor in a submarine flowline design is to ensure lateral stability against environmental loads. The most frequently used stabilization techniques in industrial practice are weight coating, trenching, and anchoring. Heavy coating negates the collapsibility of the conduit, and commercial pipeline trenching operations require heavy equipment and intensive labor at the site. These features are obviously contrary to the primary objective of expediting the military contingency operation. Therefore, securing the flowline with mechanical anchors seems to be the most practical approach for stabilization. There have been a number of extensive investigations on the stability of semirigid submarine pipeline systems (Ref 1, 2, and 3). However, highly flexible hoselines have received little attention. A direct numerical integration technique has been employed successfully to describe the catenary shape of a long cable subject to steady ocean current (Ref 4, 5, and 6). This effort was to investigate the feasibility of using the same technique to determine the behavior of a cable-like hoseline system.

SIMULATION MODEL

Problem Definition

A definition sketch of a multisegment hoseline on the ocean bottom is given in Figure 1. The hoseline may be restrained at arbitrary locations to the bottom with mechanical anchors. A pertinent free-body diagram is given in Figure 2. A right-handed coordinate system X_1, X_2, X_3 with unit orthogonal base vectors $\hat{e}_1$, $\hat{e}_2$, $\hat{e}_3$ is embedded in the bottom with $\hat{e}_3$ directed away from the ocean bottom. The vector $\hat{e}_1$ is directed outward perpendicular to the shore. The bottom is gently sloping in the $\hat{e}_1$ direction at an angle ψ with respect to the ocean surface. The gravity vector $\hat{k}$ makes an angle ψ with $\hat{e}_3$.

It is assumed that the velocity vector on the bottom is oriented in the direction of $\hat{e}_2$. There is no $\hat{e}_1$ component of the velocity vector, and its magnitude may vary in a piecewise linear fashion with X_1. The velocity is assumed to be slowly varying (i.e., at any instant a steady current will be assumed). No inertial forces will be considered. The velocity induces drag and lift forces on the hoseline. Morison-type drag forces are assumed and the independence principle is invoked to separately specify drag coefficients in the normal and tangential directions by multiplying the squares of the normal and tangent components of velocity, respectively.

The hoseline may comprise several segments joined end-to-end and forming a curved line on the bottom, with each segment having different cross-sectional properties. There are anchor points at the junctions of the segments. It is assumed that each anchor behaves as a linearly elastic spring acting in the direction of the force necessary to equalize the end-point tensions on the incident segments.

It is assumed that each segment slides on the bottom without rolling or lifting off the bottom. An analysis including the coupling between axial tension and torsional responses was beyond the scope of this work. In fact, the torsional stress, which is much smaller than that of axial tension, will not significantly affect the catenary shape of the hoseline (Ref 6). Therefore, the current-induced loads on the hose are insensitive

to the degree of twisting, as long as the hose cross section remains circular without serious buckling. Consequently, the axial and the torsional responses of the hoseline are assumed separable in this development. There is a lift force from the bottom current which tends to lift the segment, but if the segment were to separate from the bottom, the lift coefficient would decrease and the segment would be forced back into contact with the bottom, as discussed in Reference 1.

The frictional force resisting sliding of each segment is assumed to be of the Coulomb type and to be separable into components tangent and normal to the segment, with each component having a different coefficient of friction. The friction resistance is directly proportional to the magnitude of the net force normal to the seafloor by the coefficient of static friction if the segment is immobile, and by the coefficient of kinetic friction as soon as the segment moves. Typical value of the kinetic coefficient is approximately 25 percent smaller than that of the static coefficient.

Scenario of Motion

With the hoseline resting on the bottom, equilibrium can be established under zero velocity conditions. Then, as the velocity increases, a scenario of motion can be constructed as follows: (1) as the velocity increases, the drag and lift forces on the segments increase, (2) the magnitude of the reactive force from the bottom decreases and, thus, the static Coulomb friction decreases, (3) the friction force equilibrating the fluid drag forces and tensions in the curved segments increases, (4) if the friction forces in a particular segment exceed the holding capacity over a significant fraction of the segment span, the segment will move to reestablish an equilibrium position under those velocity conditions, (5) as the segment moves, the frictional force decreases in magnitude to that predicted using dynamic friction coefficients and has friction opposing the motion (i.e, in the same direction as had the static frictional resistance), (6) new locations, orientations, and tension components are established and these return the segment to equilibrium, (7) changes in the components of

tension at the end point of the segments lead to changes in the spring forces in the anchors and hence to changes in anchor locations, and (8) once new equilibrium positions of segments and anchors are established, the segments stop moving.

A new velocity magnitude can then be considered. If the velocity increases or decreases, the static frictional resistance is recomputed and compared to the holding capacity as described above.

Governing Equations

Basic Assumptions. Several basic assumptions apply throughout the derivation of this simulation model. They are:

1. The hose is uniform in shape and material along the axis of each segment length.

2. The hose is infinitely long in comparison to its diameter, and hence has no flexural stiffness.

3. The hose is pressurized and maintains a circular cross section without significant buckling.

4. The hoseline slides over the seabed without rolling if current loads exceed friction capacity of sea bottom.

Governing Equations. The hoseline system is arbitrarily located on the seafloor and subjected to gravity and nonuniform distributed current loads. Gravity acts in the direction of $\hat{k}$, which is given by:

$$\hat{k} = \psi_i \hat{e}_i \qquad (1)$$

where the summation convention on repeated indices is invoked and ψ_i is the direction cosine of $\hat{k}$. Hose behavior will be determined in terms of the location coordinates and the tension components at a material point P, which is located at an unstretched arc length S_o from origin along the hose.

Unit vectors $\hat{t}$ and $\hat{n}$, which are tangential and normal to the hoseline at P respectively, are related to the Cartesian coordinates by:

$$\hat{t} = \left(\frac{dX_\alpha}{dS}\right) \hat{e}_\alpha = \theta_\alpha \hat{e}_\alpha \qquad (2)$$

where Greek subscripts have range 1, 2, where θ_α are the direction cosines of $\hat{t}$, and dS is the stretched differential length.

$$\hat{n} = \hat{e}_3 x \hat{t} = \varepsilon_{\alpha\beta}\, \theta_\alpha\, \hat{e}_\beta \qquad (3)$$

where $\varepsilon_{\alpha\beta}$ = permutation symbol

$= 0$ if $\alpha = \beta$

$= -1$ if $\alpha > \beta$

$= 1$ if $\alpha < \beta$

Consequently, the Cartesian base vectors as expressed in terms of tangential and normal component $\hat{t}$ and $\hat{n}$ become:

$$\hat{e}_\alpha = \theta_\alpha\, \hat{t} + \varepsilon_{\beta\alpha}\, \theta_\beta\, \hat{n}$$

For a hose section, the stretched differential length dS is related to its original length dS_o by:

$$\frac{ds}{ds_o} = 1 + \varepsilon \qquad (4)$$

where ε is the strain. An elastomer hose fortified with wire or fabric reinforcements usually stretches nonlinearly under tension. The relation between elongation and axial tension is best described by empirical data. In cases where the required data are not available, the hose elongation is often approximated by:

$$\varepsilon = C_1\, T^{C_2} \qquad (5)$$

where T is axial tension magnitude, while C_1 and C_2 are material constants.

As the hose segment is assumed to have no flexural or torsional stiffness, the tension acts in the direction of unit tangent with magnitude T:

$$\bar{T} = T\, \hat{t} = T\, \theta_\alpha\, \hat{e}_\alpha = T_\alpha\, \hat{e}_\alpha$$

and components of $\bar{T}$ are:

$$T_\alpha = T\,\theta_\alpha$$

Therefore, using Equation 1, we obtain a first-order differential equation

$$\theta_\alpha = \frac{dX_\alpha}{dS} = \frac{T_\alpha}{T} \tag{6}$$

for x_α in terms of t_α and magnitude T given by:

$$T = (T_\beta \cdot T_\beta)^{1/2}$$

Replacing dS by dS_o from Equation 4, we obtain:

$$\frac{dX_\alpha}{dS_o} = (1 + \varepsilon)\,\frac{T_\alpha}{T} \tag{7}$$

Dynamic Equilibrium. From dynamic equilibrium of force vectors acting on the free body in Figure 2:

$$\left(\bar{T} + \frac{d\bar{T}}{dS}\right) - \bar{T} + \bar{F}_L\,dS + \bar{F}_B\,dS + \bar{F}_w\,dS_o + \bar{F}_D\,dS + \bar{F}_f\,dS = 0$$

where $\bar{T}$ = tension at the material point P along the hose segment

$\bar{F}_L$ = current induced lift force

$\bar{F}_D$ = current induced drag force

$\bar{F}_w$ = submerged weight per unit length of unstretched hose

$\bar{F}_B$ = sea bottom reaction normal to the seafloor

$\bar{F}_f$ = sea bottom resistance parallel to the seafloor

Canceling $\bar{T}$ and dividing by dS, we obtain:

$$\frac{d\bar{T}}{dS} + \bar{F}_L + \bar{F}_B + \bar{F}_w\left(\frac{dS_o}{dS}\right) + \bar{F}_D + \bar{F}_f = 0 \tag{8}$$

The various force vectors are developed below.

Current-Induced Forces

Velocity Vector. The current velocity acting on the hose segment in Cartesian coordinates is:

$$\bar{V} = V_\alpha \hat{e}_\alpha$$

which can be expressed in normal and tangential components as:

$$\bar{V} = \bar{V}_n + \bar{V}_t$$

where $\bar{V}_t$ = velocity tangential to segment

$\bar{V}_n$ = velocity normal to segment

Express $\bar{V}_t$ in the Cartesian coordinate system and in the tangent direction as

$$\bar{V}_t = V_{t\alpha} \hat{e}_\alpha = V_t \hat{t}$$

where

$$\bar{V}_t = (\bar{V} \cdot \hat{t}) \hat{t} = (V_\beta \theta_\beta) \hat{t}$$

Hence,

$$V_t = V_\beta \theta_\beta$$

and

$$\bar{V}_t = (V_\beta \theta_\beta)(\theta_\alpha \hat{e}_\alpha)$$

Therefore,

$$V_{t\alpha} = V_\beta \theta_\beta \theta_\alpha \qquad (9)$$

Similarly, express V_n as:

$$\bar{V}_n = V_{n\alpha} \hat{e}_\alpha = V_n \hat{n}$$

Since

$$\bar{V}_n = \bar{V} - \bar{V}_t$$

$$\bar{V}_n = V_{n\alpha}\,\hat{e}_\alpha = V_\alpha\,\hat{e}_\alpha - V_{t\alpha}\,\hat{e}_\alpha$$

Therefore,

$$V_{n\alpha} = V_\alpha - V_\beta\,\theta_\beta\,\theta_\alpha = V_\beta(\delta_{\alpha\beta} - \theta_\alpha\,\theta_\beta) \tag{10}$$

where $\delta_{\alpha\beta}$ is Kronecker delta

$$\delta_{\alpha\beta} = 0, \qquad \alpha \neq \beta, \text{ and}$$

$$\delta_{\alpha\beta} = 1, \qquad \alpha = \beta$$

Also from Equation 3:

$$\bar{V}_n = (\bar{V} \cdot \hat{n}) = (V_\eta\,\hat{e}_\eta) \cdot (\varepsilon_{\alpha\beta}\,\theta_\alpha\,\hat{e}_\eta)$$

$$= V_\beta\,\varepsilon_{\alpha\beta}\,\theta_\alpha$$

Drag, ($\bar{F}_D$). Assume that the drag force $\bar{F}_D\,dS$ can be expressed as components in the $\hat{n}$ and $\hat{t}$ directions:

$$\bar{F}_D \cdot dS = \bar{F}_{Dn} \cdot dS + \bar{F}_{Dt} \cdot dS$$

By the independence principle discussed in Reference 4, tangential components can be estimated in the same manner as normal components (Ref 1)

$$F_{Dn} = \frac{1}{2}\,\rho\,D \cdot C_{Dn}\,|V_n| \cdot V_n \tag{11a}$$

$$F_{Dt} = \frac{1}{2}\,\rho\,D \cdot C_{Dt}\,|V_t| \cdot V_t \tag{11b}$$

where C_{Dn} and C_{Dt} are normal and tangential drag coefficients. For a hose segment of practical surface, C_{Dt} is much smaller than C_{Dn}. From Equations 9 and 10, the magnitudes of $|V_t|$ and $|V_n|$ are:

$$|V_t| = (V_{t\alpha}\,V_{t\alpha})^{1/2} = (V_\beta\,V_\alpha\,\theta_\beta\,\theta_\alpha)^{1/2}$$

$$|V_n| = (V_{n\alpha}\,V_{n\alpha})^{1/2} = [V_\beta\,V_\eta\,(\delta_{\alpha\beta} - \theta_\alpha\,\theta_\beta)(\delta_{\alpha\eta} - \theta_\alpha\,\theta_\eta)]^{1/2}$$

Express the drag force F_D form of Equation 8 in Cartesian components:

$$F_{Dn} = \left(\frac{1}{2} \rho D C_{Dn}\right)(V_{n\eta} \cdot V_{n\eta})^{1/2} V_{n\alpha} \hat{e}_\alpha$$

$$F_{Dt} = \left(\frac{1}{2} \rho D C_{Dt}\right)(V_{t\eta} \cdot V_{t\eta})^{1/2} V_{t\alpha} \hat{e}_\alpha$$

where $V_{n\alpha}$ and $V_{t\alpha}$ are given by Equations 9 and 10.

Lift, ($\bar{F}_L$). F_L dS acts in the direction of $-\hat{e}_3$. Assume:

$$\bar{F}_L = -\frac{1}{2} \rho C_L D(V_\alpha V_\alpha) \hat{e}_3 \qquad (12)$$

where ρ = fluid density

D = hose diameter

C_L = lift coefficient

According to Reference 7, the lift coefficient will remain positive but will decrease as the hose separates from the bottom. The hose will repeatedly be suspended in the strong current momentarily and then fall back to the sea bottom. This situation is, however, simplified in the analysis by assuming the hose is suspended near the sea bottom, if the current is strong enough to lift the hose.

Gravity and Buoyancy (Submerged Weight, $\bar{F}_w$)

Hose weight is specified as the wet weight per unit unstretched length, w. The net gravity force exerted on the hose, $\bar{F}_w \, dS_o$, acts in the direction $\hat{k}$ and can be expressed in terms of stretched length as:

$$\bar{F}_w \, dS_o = (F_w \, dS)\left(\frac{dS_o}{dS}\right) = \frac{w \hat{k}}{1 + \varepsilon} dS$$

In Cartesian components, we replace $\hat{k}$ by Equation 1 to obtain:

$$\bar{F}_w \, dS_o = \frac{w \, dS}{1 + \varepsilon} (\psi_\alpha \hat{e}_\alpha + \psi_3 \hat{e}_3) \qquad (13)$$

Also, in normal and tangential components:

$$\bar{F}_w \, dS_o = dS (F_{w3} \hat{e}_3 + F_{wn} \hat{n} + F_{wt} \hat{t})$$

where $F_{w3} = \frac{w}{1+\varepsilon}\,\psi_3$ (14)

$$F_{wn} = \left(\bar{F}_w \frac{dS_o}{dS}\right)\cdot \hat{n} = \frac{w}{1+\varepsilon}\,\psi_\beta\,\varepsilon_{\alpha\beta}\,\theta_\alpha \quad (15)$$

$$F_{wt} = \left(F_w \frac{dS_o}{dS}\right)\cdot \hat{t} = \frac{w}{1+\varepsilon}\,\psi_\alpha\,\theta_\alpha \quad (16)$$

and θ_α is given by Equation 6 in terms of T_α/T.

Reactive Forces From the Sea Bottom

Reaction in $\hat{e}_3$ Direction, $\bar{F}_B$. As long as the hose remains in contact with the bottom, a reactive force $\bar{F}_B\,dS$ will act in the $-\hat{e}_3$ direction.

Considering equilibrium in the $\hat{e}_3$ direction, noting that $\bar{T}$ has no $\hat{e}_3$ component and using Equations 12 and 14, we obtain:

$$-\frac{1}{2}\rho\,D\,C_L\,V_\alpha\,V_\alpha - F_B + \frac{w\,\psi_3}{1+\varepsilon} = 0$$

which can be solved for F_B

$$F_B = \frac{w\,\psi_3}{1+\varepsilon} - \frac{1}{2}\rho\,D\,C_L\,V_\alpha\,V_\alpha$$

As V_α increases, F_B decreases toward $F_B = 0$, which occurs when the hose segment is lifted off the seabed.

Frictional Resistance, $\bar{F}_f$. Assuming that the friction force $\bar{F}_f\,dS$ can be taken as components in the $\hat{n}$ and $\hat{t}$ directions, and each is independently proportional to the bottom reaction force, $\bar{F}_B$, we have:

$$\bar{F}_f\,dS = \bar{F}_B\,dS\,(\mu_n\,\hat{n} + \mu_t\,\hat{t}) \quad (17)$$

where μ_n = coefficient of friction in $\hat{n}$ directions
μ_t = coefficient of friction in $\hat{t}$ directions

Signs of μ_n and μ_t are selected to oppose the tendency to move. Because of the general shape of hose segment under current loads, μ_t is assumed to be a skew-symmetric function over the segment length

$$\mu_t = \mu_{to}\left(1 - \frac{2S}{L}\right)$$

where L = span length, S = arc length from the shore end, and μ_{to} is given. Expressing Equation 17 in Cartesian components by Equations 2 and 3.

$$\bar{F}_f \, dS = \bar{F}_B \, ds(\mu_n \, \varepsilon_{\beta\alpha} + \mu_t \, \delta_{\beta\alpha}) \, \theta_\beta \, \hat{e}_\beta \qquad (18)$$

where θ_β given by Equation 6 in terms of T_β. When the segment is not moving, the static friction force F_{fs} is less than the breakout force, F_{fb}

$$|F_{fs}| \leq F_{fb} = | \, \mu_s \, F_B \, \hat{n} \, |$$

where μ_s = coefficient of static friction, with $|\mu_n|$, $|\mu_t| < \mu_s$

and the signs of μ_n, μ_t taken the same as F_{fs}. F_{fs} is determined from the static equilibrium in the normal direction as follows:

$$\bar{F}_{fs} = F_{fs} \, \hat{n} \qquad (19)$$

If the segment is not moving, the friction force equilibrates the tension gradient and other external forces in Equation 8 as long as the friction force is less than the bottom resistance capacity $\mu F_B \hat{n}$.

Thus, we consider the $\hat{n}$ components in Equation 8 to determine static friction force for comparison to the breakout force (holding capacity), $\mu_s F_B \cdot \hat{n}$. The incremental line tension $d\bar{T}/dS$ can be decomposed as follows:

$$\frac{d\bar{T}}{dS} = \left(\frac{1}{1+\varepsilon}\right)\left(\frac{d\bar{T}}{dS_o}\right) = \left(\frac{1}{1+\varepsilon}\right)\frac{d(T\,\hat{t})}{dS_o}$$

$$= \left(\frac{1}{1+\varepsilon}\right)\left[\frac{dT}{dS_o}\,\hat{t} + T\,\frac{d\hat{t}}{dS_o}\right]$$

But

$$\frac{d\hat{t}}{dS_o} = \frac{d\theta_\alpha}{dS_o}\,\hat{e}_\alpha = \frac{d}{dS_o}\left(\frac{T_\alpha}{T}\right)\hat{e}_\alpha$$

$$= \left(\frac{1}{T}\frac{dT_\alpha}{dS_o} - \frac{T_\alpha}{T^2}\frac{dT}{dS}\right)\hat{e}_\alpha = \left(\frac{1}{T}\frac{dT_\alpha}{dS_o} - \frac{T_\alpha}{T^2}\frac{dT}{dS_o}\right)(\theta_\alpha\,\hat{t} + \varepsilon_{\beta\alpha}\,\theta_\beta\,\hat{n})$$

Therefore,

$$\frac{d\bar{T}}{dS} = \left(\frac{1}{1+\varepsilon}\right)\left[\hat{t}\left(\frac{dT}{dS_o} + \frac{dT_\alpha}{dS_o}\,\theta_\alpha - \theta_\alpha\,\theta_\alpha\,\frac{dT}{dS_o}\right)\right.$$

$$\left. + \hat{n}\left(\frac{dT_\alpha}{dS_o}\,\theta_\beta - \theta_\alpha\,\theta_\beta\,\frac{dT}{dS_o}\right)\varepsilon_{\beta\alpha}\right]$$

Since $\theta_\alpha = \frac{\bar{T}_\alpha}{T}$, $\theta_\alpha\,\theta_\alpha = 1$, and $\frac{dT}{dS_o} = \frac{T_\eta}{T}\frac{dT_\eta}{dS_o}$

$$\frac{d\bar{T}}{dS} = \left(\frac{1}{1+\varepsilon}\right)\left[\hat{t}\left(\frac{T_\alpha}{T}\frac{dT_\alpha}{dS_o}\right) + \hat{n}\,\varepsilon_{\beta\alpha}\frac{T_\beta}{T}\frac{dT_\eta}{dS_o}\left(\delta_{\alpha\eta} - \frac{T_\alpha}{T}\frac{T_\eta}{T}\right)\right] \qquad (20)$$

Setting the $\hat{n}$-components in Equation 8 to zero, and using Equations 20, 14, 15, 17, and 19:

$$\hat{n}\left[\frac{\varepsilon_{\beta\alpha}}{1+\varepsilon}\frac{T_\beta}{T}\frac{dT_\eta}{dS_o}\left(\delta_{\alpha\eta} - \frac{T_\alpha}{T}\frac{T_\eta}{T}\right) + \frac{w\,\psi_\alpha}{1+\varepsilon}\,\varepsilon_{\beta\alpha}\frac{T_\beta}{T}\right.$$

$$\left. + \frac{1}{2}\,\rho\,D\,C_{Dn}(V_{n\eta}\,V_{n\eta})^{1/2}\,V_\alpha\,\varepsilon_{\beta\alpha}\frac{T_\beta}{\bar{T}} + F_{fs}\right] = 0$$

Solving for F_{fs}, assuming T_α is known, we have:

$$F_{fs} = -\,\varepsilon_{\beta\alpha}\frac{T_\beta}{T}\left[\frac{w\,\psi_\alpha}{1+\varepsilon} + \frac{1}{2}\,\rho\,D\,C_{Dn}(V_{n\eta}\,V_{n\eta})^{1/2}\,V_\alpha\right.$$

$$\left. + \frac{1}{1+\varepsilon}\frac{dT_\eta}{dS_o}\left(\delta_{\alpha n} - \frac{T_\alpha}{T}\frac{T_\eta}{T}\right)\right] \qquad (21)$$

Breakout occurs if

$$|F_{fs}| > \mu_s F_B$$

in which the sign of μ_s and F_t = sign of F_{fs}. To evaluate dT_η/dS_o in Equation 21, the actual computation uses central differences with discrete values of T_η at regularly spaced points.

Dynamic Equilibrium in $\hat{e}_\alpha$ Direction

If static breakout occurs, we replace the static friction coefficient by dynamic friction coefficient given by Equation 17 and consider equilibrium in the $\hat{e}_1$ and $\hat{e}_2$ directions. Set the $\hat{e}_\alpha$ components in Equation 8 to zero using Equations 13, 11, and 18 along with:

$$\frac{d\bar{T}}{dS} = \frac{d\bar{T}}{dS_o}\left(\frac{dS_o}{dS}\right) = \frac{d(T_\alpha \hat{e}_\alpha)}{dS_o}\left(\frac{1}{1+\varepsilon}\right) = \left(\frac{1}{1+\varepsilon}\right)\frac{dT_\alpha}{dS_o}\hat{e}_\alpha$$

Therefore, solving for dT_α/dS_o:

$$\frac{dT_\alpha}{dS_o} = -(1+\varepsilon)\left[\frac{w}{1+\varepsilon}\psi_\alpha + F_{Dt\alpha} + F_{Dn\alpha} + F_B\frac{T_\beta}{T}(\mu_n \varepsilon_{\beta\alpha} + \mu_t \delta_{\beta\alpha})\right] \quad (22)$$

where $F_{Dn\alpha} = \left(\frac{1}{2}\rho D C_{Dn}\right)(V_{n\eta} V_{n\eta})^{1/2} V_{n\alpha}$

$$V_{n\alpha} = \left(\delta_{\alpha\beta} - \frac{T_\alpha}{T}\frac{T_\beta}{T}\right)V_\beta$$

$$F_{Dt\alpha} = \left(\frac{1}{2}\rho D C_{Dt}\right)(V_{t\eta} V_{t\eta})^{1/2} V_{t\alpha}$$

$$V_{t\alpha} = \frac{T_\alpha}{T}\frac{T_\beta}{T} V_\beta$$

Thus, we must solve Equation 22 as a first order differential equation along with Equation 7, here rewritten as:

$$\frac{dX_\alpha}{dS_o} = (1+\varepsilon)\frac{T_\alpha}{T}$$

for T_α and X_α with

$$\varepsilon = C_1 T^{C_2}$$

$$T = (T_\alpha T_\alpha)^{1/2}$$

If the segment moves, we solve for the new equilibrium position and tension in which the segment ceases to move.

Numerical Solutions

Rewrite the governing Equations 7 and 22 as:

$$\frac{dX_\alpha}{dS_o} = g_{1\alpha}$$

$$\frac{dT_\alpha}{dS_o} = g_{2\alpha} + g_{3\alpha}$$

where $g_{1\alpha} = (1 + \varepsilon) \frac{T_\alpha}{T}$

$$g_{2\alpha} = -(1 + \varepsilon)\left(\frac{w \psi_\alpha}{1 + \varepsilon} + F_{Dn\alpha} + F_{Dt\alpha}\right)$$

$$g_{3\alpha} = g_{1\beta}(F_B)(\mu_n \varepsilon_{\beta\alpha} + \mu_t \delta_{\beta\alpha})$$

The solution to these nonlinear equations can be obtained by iteration on quasi-linearized equations. Taking Taylor expansions of $g_{i\alpha}$, $i = 1,3$, we can use the Newton-Raphson iteration method as described in Reference 8:

$$\frac{dX_\alpha}{dS_o} = \tilde{g}_{1\alpha} + a_{1\alpha\beta}(T_\alpha - \tilde{T}_\alpha)$$

$$\frac{dT_\alpha}{dS_o} = \tilde{g}_{2\alpha} + \tilde{g}_{3\alpha} + (a_{2\alpha\beta} + a_{3\alpha\beta})(T_\beta - \tilde{T}_\beta)$$

where $\tilde{g}_{i\alpha} = g_{i\alpha}\Big|_{\tilde{X}_\eta, \tilde{T}_\eta}$

$$a_{i\alpha\beta} = \left[\frac{\partial g_{i\alpha}}{\partial T_\beta}\right]_{\tilde{X}_\eta, \tilde{T}_\eta}$$

$\tilde{X}_\eta, \tilde{T}_\eta$ = approximated values

The iterative process proceeds as follows: assume values $\tilde{X}_\alpha$ and $\tilde{T}_\alpha$ at each point, calculate $\tilde{g}_{i\alpha}$ and $\tilde{a}_{i\alpha\beta}$, and solve the linearized equation for improved answer X_α and T_α. Repeat this iterative process until $(X_\alpha - \tilde{X}_\alpha)$ and $(T_\alpha - \tilde{T}_\alpha) \doteq 0$.

PARAMETRIC ANALYSIS

Parameters Considered in the Test

A sensitive analysis was conducted to investigate the influence on the hoseline response of the governing parameters considered in the simulation model. The parameters tested include four categories: (1) the axial rigidity of the hose, (2) the hoseline geometry, (3) the current velocity, and (4) the seabed resistance. Tests were conducted by varying one parameter at a time while keeping the others constant. A wide range of hose rigidity was tested for the influence of rigidity. However, only a rigid hose was used in the rest of the numerical experiments in order to separate the effect of other parameters from the influence of hose elongation.

Axial Rigidity of the Hose

High-strength hoses are often made of elastomers fortified with steel or synthetic fiber reinforcement. Their axial rigidities depend on the material and the construction of their reinforcements. These

hoses usually stretch nonlinearly under tension as shown in Figure 3. The data presented in Figure 3 were obtained from an elongation test of a highly stretchable hose (Ref 9). The age and the previous loading history of the hose may also change the axial rigidity significantly. Therefore, it is rather difficult to accurately estimate the rigidity of a hose. A numerical test was conducted to examine the influence of the rigidity on the behavior of a hoseline. In order to study the effect in general, the rigidity is represented by a load deflection relation approximated by Equation 5. The influence of the material coefficients, C_1 and C_2, were tested separately. The test was first conducted using a hose of linear material. In this case, C_2 is unity and C_1 is directly related to the modulus of elasticity. A wide range of C_1, which represents conduits varying from a steel pipe to a highly stretchable rubber hose, was tested. Figures 4a and 4b present the lateral deflection and the hose tension, respectively. Both are nondimensionalized by their corresponding values of an unstretchable hose, which has a modulus of elasticity equal to E_{steel}. E_{hose} and E_{steel} represent the modulae of elasticity of the hose and steel, respectively. S/L denotes the segment length-to-span ratio. The results indicated that the response of a tight segment with small S/L ratio to a strong current is heavily influenced by the rigidity of the hose. This fact is especially true when the equivalent modulus of elasticity is less than one thousandth of E_{steel}. It is important to note that the rigidity of a typical submarine hose is within this range. A highly stretchable hose in a strong current elongates extensively and develops a deeper curved shape than would a rigid hose with the same initial S/L ratio. Therefore, the tension load and the lateral deflection of a tight stretchable segment in a strong current may increase as much as 300 percent, if improper hose rigidity were used. On the other hand, the response of a tight or loose segment in moderate currents appears to be much less sensitive to the variation of the rigidity. The axial tension remains nearly constant over a wide range of the rigidity. The reason can be attributed to the effect of the equilibrium shape of the segment on the hose response, which will be described in the test of

hoseline geometry. Figure 5 summarizes the effect of the material coefficient C_2. The value of C_2 reflects the stiffening process of the reinforcement of a hose. For a realistic hose, C_2 is generally less than unity. Again, the influence of C_2 becomes important only when the hose is heavily loaded beyond the extent that the hose begins stiffening. This occurs when a tight hose is installed in a strong current.

Current Force

The current-induced force on a hose section is a function of the current velocity, the current direction, the hose diameter, and the hydrodynamic coefficients. This simulation model employs the Morison equation to estimate the current force. Therefore, the current forces can be expected to be proportional to the hose diameter and the hydrodynamic coefficients. If the curved shape of the hose segment remains the same, the force should be proportional to the normal velocity squared. This relation was verified by the results presented in Figure 6. The hose tension, due to a broadside current, follows a parabolic function closely, as long as the current is strong enough to overcome the seabed resistance. The influence of the current direction on the hose response is more complicated, because the segment changes its equilibrium shape in compliance with the current direction, as shown in Figure 7. A hose section oblique to the current direction experiences a much larger reduction in form drag than the increase in skin drag. As a result, the total current force exerted on the section decreases significantly. Figure 8 summarizes the anchor loads on three segments of different S/L ratios in various current directions. The forces are nondimensionalized by the forces due to broadside currents. Generally, the anchor loads decrease in a form of $\text{Cos}^n\theta$ as the current shifts away from the direction normal to the hose length. The angle is defined in Figure 9. The value of n decreases as the S/L ratio of the segment increases. Since the hose is fairly stiff and stretches very little, the result reflects the influence of the current direction alone. Considering a segment of S/L = 1.0, the segment remains straight irrespective of the current direction. The anchor load can be expected to be proportional to the normal velocity

squared (i.e., $V_c^2 \cos^2\theta$), which is confirmed by the results of the case of S/L = 1.01. On the other hand, a loose segment aligns a large portion of its length with the current, and therefore experiences less cross current. As a result, the effect of the current diminishes.

Hoseline Geometry

The equilibrium shape of a hose segment determines the orientation of the hose section with respect to the current, and therefore significantly affects the total current applied on a hoseline. Intuitively, a loose segment tends to align a larger portion of its length with the current direction, and therefore experiences a smaller current force than a tight segment. The curved shape of a flexible tension member subject to a uniform load can be uniquely characterized by the ratio of the segment length, S, to the span distance, L. Consequently, the S/L ratios were selected to represent the geometry of a hoseline segment. Figure 10 summarizes the influence of the hoseline geometry on the hoseline behavior. Values of S/L were generated by using different combinations of various span distances and various segment lengths. The hoseline responses in 1.5- and 4.0-knot broadside currents were tested. The results clearly demonstrate that the response of a hose segment of little stretchability is determined solely by the S/L ratio and is linearly proportional to the segment length and the span distance. In general, the hoseline response remains roughly constant for a S/L ratio greater than 1.2, and increases rapidly when the ratio decreases below 1.2. Since an unstretchable hose is used in this test, the lateral deflection is not sensitive to the current velocity and the line tension and the anchor load are closely proportional to the velocity squared, as anticipated.

Sea Bottom Resistance

Seabed resistance depends on the combination of the unit weight of conduit, the lifting force, and the soil properties. The soil reaction is more complicated and less understood than other parameters involved.

The mechanism of the soil reaction is approximated with a Coulomb friction force. All the factors involved are included in a simple friction coefficient. Friction coefficients varying from 0.3 to 0.9, which represent a typical hard sandy seabed, were tested to show the influence on the hose response. The tests were repeated for conduits of unit weights from 3 to 7 pounds per linear foot in a 1.5-knot current. Unfortunately, the results shown in Figure 11 are not conclusive. Further research efforts are required to identify the influence of the sea bottom resistance. However, the typical submarine hoses are usually light and are likely to be lifted off the sea bottom by a moderate current. Therefore, the influence of the bottom resistance may be negligible.

STABILITY OF NAVY HOSELINE

A three-segment hoseline secured with four anchors equally spaced along a straight line on a flat horizontal seabed was used to show the stability, in general, of a Navy hoseline. Stability was evaluated in terms of the maximum lateral deflection, the maximum tension, and the anchor loads. Calculations were conducted for two hoses of various layouts in the current environment of practical application. The results were compiled in a series of design charts.

Characteristics of Navy Hoses

Figure 3 demonstrates the behavior of a typical Navy submarine fuel hose under tension. This particular hose is made of synthetic rubber fortified with 2-ply contra helical steel wire reinforcements. Figure 3a relates the axial elongation and the variation in outside diameter of the hose to the axial tension. The hose stretches linearly at low tension, and becomes highly nonlinear as the tension exceeds 20 kips. This fact can be attributed to the two distinct deformation mechanisms of the hose reinforcements at different load levels. At low tension, the helical wire reinforcement stretches like a regular helical spring without actually deforming the wire material. Therefore, the hose is fairly flexible and

a linear relation between load and deflection can be expected. As the axial tension exceeds the magnitude which rotates the lay angle of the reinforcement wire to the limit, the wire begins stretching itself to resist the external loads. The hose becomes much more stiff and highly nonlinear thereafter. Another remarkable feature of the Navy hoses, along with their high stretchability, is their extensive diameter reduction. Figure 3c shows that the outside diameter of the hose reduces almost the same amount as the axial elongation in percentage of their original dimension. Furthermore, the results from a simple calculation based on the data presented in Figure 3 indicate that the wall thickness of the hose changes very little when the hose stretches (Appendix B). Reduction in hose size is due to contraction of the inner diameter. The reduction in hose diameter has to be properly accounted for in the calculation of current loads experienced by the hose segments. The axial stiffness of the hose is also dependent on the pressure inside the hose. High internal pressure resists the radial contraction of the hose reinforcement layer. This makes the reinforcement layer harder to stretch, as for a helical spring. As a result, the hose becomes stiffer when the pressure inside the hose increases, as shown in Figure 3(b). Therefore, the empirical load deflection curve of the hose measured under working internal pressure shall be used for the final design.

Hose Layouts. The calculation was repeated for two hoses of different axial rigidity. One is the highly stretchable Navy hose described in the previous section. The other is a rigid hose of a very little stretchability. Hoses that were 7.5 and 9.5 inches in outside diameter were used. The segment lengths of 200, 500, 1,000, and 2,000 feet were included in the calculation. The segment length in combination with different span distance between anchors results in various S/L ratios from 1.05, 1.10, 1.15, and 1.20.

Environmental Conditions. The hoseline stability was calculated for the currents approaching from 0, 15, and 30 degrees off the perpendicular to the general direction of the hoseline. Six different

current speeds in the 0.5- to 4-knot range were used for each current direction. The hydrodynamic coefficients for a submarine flowline vary significantly from case to case. Their values depend on the experiment setup, model scale, current condition, data acquisition procedure, and data reduction method. Generally, these force coefficients are valid only for conditions similar to those for which they were measured. The inline drag coefficients used in the contemporary engineering practice vary from 0.75 to 1.40. The transverse drag coefficients vary from 0.6 to 1.0. The low values were empirical data measured in 37 feet of water offshore Honolulu (Ref 10), whereas the high values were recommended by Det Norske Veritas for designing a submarine pipeline system (Ref 11). Both sets are for steel or concrete coated steel pipes. Data for synthetic rubber hoses are not available. However, practical hoses are much smaller than the thickness of the boundary layer of the water current, and are therefore fully submerged in the boundary layer. Consequently, the actual current velocity experienced by the hoses is smaller than that of the free stream. Using the lower force coefficients in combination with the free stream velocity seems to be more realistic. Navy hoseline is a relocatable system intended for worldwide application. The system may be installed on various types of sea bottoms. Field data show that the typical Coulomb friction coefficient for a steel or concrete pipe on a hard sandy seabed varies from 0.3 to 0.9 (Ref 5). A low friction coefficient of 0.3, which will result in higher loads, was used in the calculation. The hose particulars and the environmental conditions are summarized in Table 1.

Results

A total of eight design charts (Tables 2 through 5) were prepared for various hose rigidities, hose particulars, and current conditions. The results for the rigid hose (Tables 2 and 3) were further reduced into a parametric model, Equations 23 through 26, using the findings obtained from the parametric analysis as a guideline. The parametric model is compared with the complete simulation model in Figure 12. The

solid lines indicate two models with identical results. The parametric model provides a good approximation for the conditions within the limits indicated:

$$\frac{d}{L} = 0.07\ (SDV_n)^{0.05}\ (\frac{S}{L})^{6} \qquad (23)$$

$$\frac{T_m}{L} = 0.17\ D\ V_n^{\ 2}\ (\frac{S}{L})^{-4} \qquad (24)$$

$$\frac{A_e}{L} = 0.17\ D\ V_n^{\ 2}\ (\frac{S}{L})^{-4} \qquad (25)$$

$$\frac{A_i}{L} = 0.25\ D\ V_n^{\ 2}\ (\frac{S}{L})^{-4} \qquad (26)$$

where d = deflection (ft)
T_m = maximum hose tension (lb)
A_e = current load at end anchors (lb)
A_i = current load at intermediate anchors (lb)
L = span distance between anchors (ft)
S = segment length between anchors (ft)
V_n = normal component of current velocity (knots)
D = outside diameter of the hose (in.)

Limits:

$5 \leq D \leq 10$ inches $\qquad 200 \leq S \leq 2{,}000$ feet
$1 \leq V_n \leq 4$ knots $\qquad 1.05 \leq S/L \leq 1.20$

Engineering Applications

ACP Hose. The stability of the Advanced Collapsible Pipe hose can be evaluated directly by using the design charts. It is assumed that a 6-inch ACP hose is to be installed in a uniform 2-knot cross current. The outside diameter of the hose is approximately 7.5 inches. It is further assumed that the system is to be installed at an initial (or unstretched) segment length-to-span ratio of 1.05. The anchor capacity

required to hold a hose segment of various lengths against a 2-knot broadside current can be obtained from Table 3 under the column labelled with '0 degree' and 'Anchor load.' Columns (1) and (2) give the current loads at the end and the intermediate anchors, respectively. For example, the minimum holding capacity of the anchor at the end of a 1,000-foot segment can be obtained from the row labelled with S/L = 1.05, Length = 1000, and V = 2.0. The results are 3.2 and 4.2 kips for the end and the intermediate anchor, respectively. As a matter of fact, there is more than one way to anchor a hoseline. Final selection requires a trade-off analysis taking into consideration of the strength of the hose, the lateral deflection, the holding capacity of the anchors, the installation requirements, and the operation costs, etc.

Other Hoses. The stability of other hoses, whose axial rigidities are substantially different than those of the ACP hose, may be determined by iteration using the design charts for the rigid hose along with the empirical load deflection relation of the hose under consideration. The iteration procedure includes four simple steps: (1) determine the hose tension from the proper design chart for the rigid hose using the initial (unstretched) S/L ratio and other given parameters, (2) determine the elongation, ε, associated with that tension from the empirical load deflection relation, and (3) calculate the new S/L ratio by multiplying the old S/L by $(1+\varepsilon)$. Then, (4) use the new S/L ratio and repeat steps 1 to 3 until the tension load comes within desired tolerance. For example, the stability of the ACP hose demonstrated in the previous paragraph can also be determined using the design charts for rigid hoses. Step 1: Entering Table 2 with S/L = 1.05, V = 2.0, S = 1,000, and θ = 0 degree, the tension load is 4.5 kips. Step 2: Interpolating from Figure 3, the elongation of the hose under 4.5 kips tension is 7 percent. Step 3: The new S/L ratio is therefore equal to 1.12. Repeating steps 1 to 3 with the new S/L ratio, the second iteration gives a tension of 2.8 kips and a elongation of 5 percent. The third iteration gives a tension of 3.1 kips and an elongation of 5 percent, which are within the accuracy of the design charts. Therefore, the equilibrium S/L ratio of the segment is 1.05 X (1+0.05) = 1.10. The loads at the end and the intermediate

anchors are determined from Table 1, with S/L = 1.10 and S = 1,050 feet, as 3.2 and 4.2 kips, respectively. The results are identical with those obtained directly from the design charts for ACP hoses. Furthermore, the stability of a rigid hose can also be determined from the parametric model, Equations 23 through 26. Equation 24 is used in place of design charts for estimating the tension loads, and Equations 23, 25, and 26 are used to determined the lateral deflection and the anchor loads. The iteration procedure remains the same.

CONCLUSIONS

1. The lateral stability of a flexible submarine hoseline on the sea-floor in a slowly varying current environment may be properly simulated based on the Morison equation and a nonlinear cable theory. Stability can be evaluated in terms of anchor load, axial tension, and maximum lateral deflection of the hoseline.

2. The on-bottom behavior of the hoseline is most influenced by the following factors: the equilibrium curved shape of the hose segment, the size of hose, the current velocity, and the axial rigidity of the hose. The influence of the sea bottom resistance is negligible from a design point of view.

3. The equilibrium curved shape of a hose segment, which may be represented by the segment length-to-span ratio, S/L, is the most dominant factor on the response of a hoseline. The influence of S/L on the responses is illustrated in Figure 10. The results show that a tight hose segment with a small S/L ratio will experience large current loads with small lateral deflection, and that a loose hose with a large S/L ratio will experience a smaller current load, but with a much larger lateral deflection. A proper S/L ratio has to be selected according to the capacity of anchors, the strength of the hose, and the operational requirements. A ratio between 1.05 and 1.10 is recommended for practical applications based on the results of a parametric analysis.

4. At a constant equilibrium S/L ratio, the load is proportional to the hose size, the hydrodynamic coefficients, and the span distance, and is closely proportional to the normal current velocity squared.

5. The axial rigidity influenced the elongation of a hose segment, and hence the equilibrium S/L ratio. The influence is significant for a tight stretchable hose segment deployed in a fast current, and is negligible for other cases such as a loose hose of little to moderate stretchability deployed in a slow current.

6. The optimum segment geometry of a simple hoseline may be determined by iteration using the design charts provided in Tables 2 to 5 or the parametric model described by Equations 23 to 26. The iteration procedures are demonstrated in the section on Engineering Applications. The simulation program, NCELHOSE, is recommended for the analysis of a more complicated hoseline. The source code and assistance to use the program are available at NCEL.

REFERENCES

1. T. Sarpkaya, and M.ST.Q. Isaacson. Mechanics of wave forces on offshore structures. New York, NY, Van Nostrand Reinhold Co., 1981.

2. M.C. Huang, and R. T. Hudspeth. "Pipeline stability under finite amplitude waves," Journal of Waterway, Port, Coastal, and Ocean Division, ASCE, vol 108, no. WW2, May 1982, pp 125-145.

3. K. Holthe, T. Sotberg, and J. C. Chao. "An efficient computer model for predicting submarine pipeline response to waves and current," in Proceedings of the Offshore Technology Conference, Houston, TX, Apr 1987, Paper No. 5502, pp 159-169.

4. Y.I. Choo, and M.S. Casarella. "Configuration of a towline attached to a vehicle moving in a circular path," Journal of Hydronautics, vol 6, 1972, pp 51-57.

5. R.B. Chiou. Nonlinear static analysis of long submerged cable segment by spatial integration, M.S. Report, Oregon State University, Corvallis, OR, Jul 1987.

6. R.C. Simpson, and J. W. Leonard. Long cables under steady ocean load with coupled tension/torsion, Report No. OE-87 51, Oregon State University, Corvallis, OR, 1987.

7. J. Fredsoe, and E. A. Hansen. "Lift forces on pipelines in steady flow," Journal of Waterway, Port, Coastal, and Ocean Engineering, vol 113, no. 2, 1987.

8. J.W. Leonard. Tension structures. New York, NY, McGraw-Hill Book Company, 1988.

9. J.P. Harrell. First article performance testing of the Uniroyal Manuli Offshore Patroleum Discharge Fuel conduit, vol 1, Southwest Research Institute, San Antonio, TX, Apr 1988.

10. R.A. Grace, et al. "Hawaii ocean test pipe project: force coefficients," in Proceedings of the Civil Engineering in Ocean IV, Sep 1979, pp 99-110.

11. Det Norske Veritas. Rules for submarine pipeline systems. Veritasveien 1, 1322 Hovik, Norway, 1981.

Table 1. Range of Parameters Used to Generate Design Charts

Parameter	Range
Hose Diameter	
Outer	7.5 and 9.5 inches
Inner	6.0 and 8.0 inches
Hoseline Geometry	
Length	200, 500, 1,000 and 2,000 feet
S/L	1.05, 1.10, 1.15, and 1.20
Current Velocity	
Magnitude	0.5, 1.0, 1.5, 2.0, 3.0, and 4.0 knots
Direction	0, 15, and 30 degrees
Hydrodynamic Force Coefficients	
C_D	0.75
C_L	0.60
C_t	0.1
Friction Coefficients	
Static	0.3
Dynamic	0.25

Table 2. Response of rigid hoseline to steady currents (Do = 7.5 inches, Di = 6.0 inches, Wet = 5 lb/ft, C_D = 0.75, C_L = 0.6, C_f = 0.3)

RIGID

S/L	Length (feet)	V (kts)	0 degree						15 degrees						30 degrees					
			max. defl. (feet)		axial ten. (Kips)		anchor load (Kips)		max. defl. (feet)		axial ten. (Kips)		anchor load (Kips)		max. defl. (feet)		axial ten. (Kips)		anchor load (Kips)	
			(1)	(2)	(1)	(2)	(1)	(2)	(1)	(2)	(1)	(2)	(1)	(2)	(1)	(2)	(1)	(2)	(1)	(2)
1.05	200	0.5	25	25	0.0	0.0	0.0	0.0	26	26	0.0	0.0	0.0	0.0	26	27	0.0	0.0	0.0	0.0
1.05	200	1.0	25	25	0.0	0.0	0.0	0.0	26	26	0.0	0.0	0.0	0.0	26	27	0.0	0.0	0.0	0.0
1.05	200	1.5	27	27	0.4	0.4	0.4	0.4	26	26	0.4	0.4	0.4	0.4	26	26	0.3	0.3	0.3	0.3
1.05	200	2.0	27	27	0.9	0.9	0.9	0.9	26	26	0.9	0.9	0.9	0.8	27	26	0.7	0.7	0.7	0.7
1.05	200	3.0	27	27	2.1	2.1	2.1	2.1	26	26	2.0	2.0	2.0	2.0	27	26	1.7	1.7	1.7	1.6
1.05	200	4.0	27	27	3.7	3.7	3.7	3.7	26	26	3.5	3.6	3.5	3.5	27	26	3.0	3.0	3.0	2.9
1.05	500	0.5	65	65	0.0	0.0	0.0	0.0	66	65	0.0	0.0	0.0	0.0	66	65	0.0	0.0	0.0	0.0
1.05	500	1.0	65	65	0.0	0.0	0.0	0.0	66	65	0.0	0.0	0.0	0.0	66	65	0.0	0.0	0.0	0.0
1.05	500	1.5	66	66	1.0	1.0	1.0	1.0	66	66	0.9	0.9	0.9	0.9	65	65	0.7	0.7	0.7	0.7
1.05	500	2.0	66	66	2.3	2.3	2.2	2.2	66	66	2.1	2.1	2.1	2.1	65	66	1.8	1.8	1.8	1.7
1.05	500	3.0	66	66	5.3	5.3	5.3	5.3	66	67	5.0	5.0	5.0	4.9	66	66	4.2	4.2	4.2	4.1
1.05	500	4.0	66	66	9.3	9.4	9.3	9.3	66	67	8.8	8.9	8.9	8.8	66	66	7.4	7.4	7.4	7.3
1.05	1000	0.5	132	132	0.1	0.1	0.1	0.1	132	132	0.1	0.1	0.1	0.1	132	132	0.1	0.1	0.1	0.1
1.05	1000	1.0	132	132	0.1	0.1	0.1	0.1	132	132	0.1	0.1	0.1	0.1	132	132	0.1	0.1	0.1	0.1
1.05	1000	1.5	133	133	2.0	2.0	2.0	1.9	133	133	1.9	1.9	1.8	1.8	130	131	1.4	1.4	1.4	1.4
1.05	1000	2.0	133	133	4.5	4.5	4.5	4.5	133	133	4.3	4.3	4.3	4.2	132	131	3.5	3.5	3.5	3.5
1.05	1000	3.0	133	133	10.5	10.5	10.5	10.5	134	133	10.0	10.0	10.0	9.9	132	132	8.3	8.3	8.3	8.2
1.05	1000	4.0	134	134	18.6	18.6	18.6	18.7	134	133	17.6	17.7	17.6	17.6	132	133	14.7	14.7	14.7	14.6
1.05	2000	0.5	265	265	0.2	0.2	0.2	0.2	265	264	0.2	0.2	0.2	0.2	265	265	0.1	0.1	0.1	0.1
1.05	2000	1.0	265	265	0.2	0.2	0.2	0.2	265	264	0.2	0.2	0.2	0.2	265	265	0.1	0.1	0.1	0.1
1.05	2000	1.5	267	267	4.1	4.1	3.9	3.8	265	265	3.8	3.8	3.6	3.6	260	261	2.9	2.9	2.8	2.7
1.05	2000	2.0	267	267	9.0	9.0	9.0	9.0	267	267	8.5	8.5	8.5	8.4	264	264	7.0	7.0	7.0	6.9
1.05	2000	3.0	269	269	20.9	20.9	20.9	21.0	269	269	19.8	19.9	19.8	19.8	265	265	16.5	16.5	16.5	16.4
1.05	2000	4.0	271	271	36.9	37.0	36.9	37.3	271	270	35.0	35.1	35.0	35.1	267	267	29.2	29.3	29.2	29.1
1.10	200	0.5	36	36	0.0	0.0	0.0	0.0	36	36	0.0	0.0	0.0	0.0	36	36	0.0	0.0	0.0	0.0
1.10	200	1.0	36	36	0.0	0.0	0.0	0.0	36	36	0.0	0.0	0.0	0.0	36	36	0.0	0.0	0.0	0.0
1.10	200	1.5	36	36	0.3	0.3	0.3	0.3	36	36	0.3	0.3	0.2	0.3	35	35	0.2	0.2	0.2	0.2
1.10	200	2.0	36	36	0.6	0.6	0.6	0.8	35	36	0.6	0.6	0.6	0.7	35	36	0.5	0.5	0.5	0.6
1.10	200	3.0	36	36	1.5	1.5	1.5	1.9	35	36	1.4	1.4	1.4	1.8	35	36	1.2	1.2	1.2	1.5
1.10	200	4.0	36	36	2.6	2.6	2.6	3.3	35	36	2.5	2.5	2.5	3.1	35	36	2.1	2.1	2.1	2.7
1.10	500	0.5	91	91	0.0	0.0	0.0	0.0	91	91	0.0	0.0	0.0	0.0	91	91	0.0	0.0	0.0	0.0
1.10	500	1.0	91	91	0.0	0.0	0.0	0.0	91	91	0.0	0.0	0.0	0.0	91	91	0.0	0.0	0.0	0.0
1.10	500	1.5	92	92	0.7	0.7	0.6	0.8	91	91	0.6	0.6	0.6	0.8	88	88	0.5	0.5	0.5	0.6
1.10	500	2.0	91	91	1.5	1.5	1.5	2.0	90	91	1.5	1.5	1.5	1.9	89	89	1.2	1.2	1.2	1.6
1.10	500	3.0	91	91	3.6	3.6	3.6	4.7	90	91	3.5	3.5	3.5	4.4	89	90	2.9	2.9	2.9	3.7
1.10	500	4.0	92	92	6.4	6.4	6.4	8.3	91	91	6.2	6.2	6.2	7.9	89	90	5.2	5.2	5.2	6.6
1.10	1000	0.5	182	182	0.1	0.1	0.1	0.1	182	182	0.1	0.1	0.1	0.1	182	182	0.0	0.0	0.0	0.1
1.10	1000	1.0	182	182	0.1	0.1	0.1	0.1	182	182	0.1	0.1	0.1	0.1	182	182	0.0	0.0	0.0	0.1
1.10	1000	1.5	183	183	1.4	1.4	1.3	1.6	181	183	1.3	1.3	1.2	1.5	176	176	1.0	1.0	1.0	1.2
1.10	1000	2.0	183	183	3.1	3.1	3.1	4.0	182	181	2.9	2.9	2.9	3.7	178	178	2.5	2.5	2.5	3.1
1.10	1000	3.0	183	183	7.2	7.2	7.2	9.4	182	182	6.9	6.9	6.9	8.8	179	178	5.9	5.9	5.9	7.5
1.10	1000	4.0	183	183	12.9	12.9	12.9	16.6	182	182	12.3	12.3	12.3	15.7	179	179	10.4	10.5	10.4	13.3
1.10	2000	0.5	364	364	0.1	0.1	0.1	0.2	363	364	0.1	0.1	0.1	0.2	364	363	0.1	0.1	0.1	0.1
1.10	2000	1.0	364	364	0.1	0.1	0.1	0.2	363	364	0.1	0.1	0.1	0.2	364	363	0.1	0.1	0.1	0.1
1.10	2000	1.5	367	367	2.7	2.7	2.6	3.3	364	365	2.5	2.5	2.4	3.0	353	353	2.0	2.0	1.9	2.3
1.10	2000	2.0	366	366	6.2	6.2	6.2	7.9	364	364	5.9	5.9	5.9	7.5	358	358	4.9	4.9	4.9	6.2
1.10	2000	3.0	368	368	14.5	14.5	14.5	18.7	366	365	13.9	13.9	13.9	17.7	358	359	11.8	11.8	11.8	14.9
1.10	2000	4.0	368	368	25.6	25.7	25.7	33.2	367	366	24.6	24.6	24.6	31.4	360	359	20.9	20.9	20.9	26.5

Table 2. Continued

RIGID

S/L	Length (feet)	V (kts)	0 degree						15 degrees						30 degrees					
			max. defl. (feet)		axial ten. (Kips)		anchor load (Kips)		max. defl. (feet)		axial ten. (Kips)		anchor load (Kips)		max. defl. (feet)		axial ten. (Kips)		anchor load (Kips)	
			(1)	(2)	(1)	(2)	(1)	(2)	(1)	(2)	(1)	(2)	(1)	(2)	(1)	(2)	(1)	(2)	(1)	(2)
1.15	200	0.5	43	43	0.0	0.0	0.0	0.0	42	43	0.0	0.0	0.0	0.0	43	43	0.0	0.0	0.0	0.0
1.15	200	1.0	43	43	0.0	0.0	0.0	0.0	42	43	0.0	0.0	0.0	0.0	43	43	0.0	0.0	0.0	0.0
1.15	200	1.5	44	44	0.2	0.2	0.2	0.3	43	43	0.2	0.2	0.2	0.3	42	42	0.2	0.2	0.2	0.2
1.15	200	2.0	43	43	0.5	0.5	0.5	0.7	43	43	0.5	0.5	0.5	0.7	42	43	0.4	0.4	0.4	0.6
1.15	200	3.0	42	43	1.2	1.2	1.2	1.7	43	43	1.1	1.1	1.1	1.6	43	43	1.0	1.0	1.0	1.4
1.15	200	4.0	44	43	2.1	2.1	2.1	3.0	43	43	2.0	2.0	2.0	2.8	43	43	1.7	1.7	1.7	2.4
1.15	500	0.5	108	108	0.0	0.0	0.0	0.0	108	108	0.0	0.0	0.0	0.0	108	108	0.0	0.0	0.0	0.0
1.15	500	1.0	108	108	0.0	0.0	0.0	0.0	108	108	0.0	0.0	0.0	0.0	108	108	0.0	0.0	0.0	0.0
1.15	500	1.5	109	109	0.5	0.5	0.5	0.7	108	109	0.5	0.5	0.5	0.7	103	104	0.4	0.4	0.4	0.5
1.15	500	2.0	109	109	1.2	1.2	1.2	1.8	108	108	1.2	1.2	1.2	1.7	105	106	1.0	1.0	1.0	1.4
1.15	500	3.0	109	109	2.9	2.9	2.9	4.2	108	108	2.8	2.8	2.8	4.0	105	106	2.4	2.4	2.4	3.4
1.15	500	4.0	109	109	5.1	5.1	5.1	7.5	108	108	5.0	5.0	5.0	7.1	105	106	4.3	4.3	4.3	6.1
1.15	1000	0.5	216	216	0.1	0.1	0.1	0.1	216	216	0.1	0.1	0.1	0.1	217	216	0.0	0.0	0.0	0.1
1.15	1000	1.0	216	216	0.1	0.1	0.1	0.1	216	216	0.1	0.1	0.1	0.1	217	216	0.0	0.0	0.0	0.1
1.15	1000	1.5	219	219	1.1	1.1	1.0	1.4	217	217	1.0	1.0	0.9	1.3	207	207	0.8	0.8	0.8	1.0
1.15	1000	2.0	218	218	2.4	2.4	2.4	3.6	217	217	2.4	2.4	2.4	3.4	210	210	2.0	2.0	2.0	2.8
1.15	1000	3.0	218	218	5.8	5.8	5.8	8.4	216	216	5.6	5.6	5.6	8.0	211	211	4.8	4.8	4.8	6.8
1.15	1000	4.0	218	218	10.3	10.3	10.3	15.0	217	217	9.9	9.9	9.9	14.2	212	211	8.5	8.5	8.5	12.1
1.15	2000	0.5	432	432	0.1	0.1	0.1	0.2	433	433	0.1	0.1	0.1	0.2	433	433	0.1	0.1	0.1	0.1
1.15	2000	1.0	432	432	0.1	0.1	0.1	0.2	433	433	0.1	0.1	0.1	0.2	433	433	0.1	0.1	0.1	0.1
1.15	2000	1.5	438	438	2.1	2.1	2.0	2.8	434	434	1.9	1.9	1.9	2.6	415	415	1.5	1.5	1.5	2.0
1.15	2000	2.0	436	436	4.9	4.9	4.9	7.1	432	433	4.7	4.7	4.7	6.7	422	422	4.0	4.0	4.0	5.7
1.15	2000	3.0	437	437	11.5	11.5	11.5	16.9	433	434	11.1	11.1	11.1	16.0	423	423	9.6	9.6	9.6	13.6
1.15	2000	4.0	437	437	20.5	20.5	20.5	30.0	434	434	19.8	19.8	19.8	28.5	424	423	17.1	17.1	17.1	24.3
1.20	200	0.5	48	48	0.0	0.0	0.0	0.0	48	48	0.0	0.0	0.0	0.0	48	48	0.0	0.0	0.0	0.0
1.20	200	1.0	48	48	0.0	0.0	0.0	0.0	48	48	0.0	0.0	0.0	0.0	48	48	0.0	0.0	0.0	0.0
1.20	200	1.5	49	49	0.2	0.2	0.2	0.2	48	48	0.2	0.2	0.2	0.2	46	46	0.1	0.1	0.1	0.2
1.20	200	2.0	49	49	0.4	0.4	0.4	0.6	48	48	0.4	0.4	0.4	0.6	47	47	0.3	0.3	0.3	0.5
1.20	200	3.0	48	48	1.0	1.0	1.0	1.5	48	47	1.0	1.0	1.0	1.5	47	47	0.8	0.8	0.8	1.3
1.20	200	4.0	48	49	1.7	1.7	1.7	2.7	48	47	1.7	1.7	1.7	2.6	47	47	1.5	1.5	1.5	2.2
1.20	500	0.5	122	122	0.0	0.0	0.0	0.0	121	121	0.0	0.0	0.0	0.0	121	121	0.0	0.0	0.0	0.0
1.20	500	1.0	122	122	0.0	0.0	0.0	0.0	121	121	0.0	0.0	0.0	0.0	121	121	0.0	0.0	0.0	0.0
1.20	500	1.5	123	123	0.4	0.4	0.4	0.6	121	121	0.4	0.4	0.4	0.6	116	116	0.3	0.3	0.3	0.4
1.20	500	2.0	122	122	1.0	1.0	1.0	1.6	121	121	1.0	1.0	1.0	1.5	118	117	0.9	0.9	0.9	1.3
1.20	500	3.0	122	122	2.4	2.4	2.4	3.9	121	121	2.4	2.4	2.4	3.7	118	117	2.1	2.1	2.1	3.1
1.20	500	4.0	122	122	4.4	4.4	4.4	6.9	121	121	4.2	4.2	4.2	6.5	118	117	3.7	3.7	3.7	5.6
1.20	1000	0.5	243	243	0.1	0.1	0.1	0.1	243	243	0.0	0.0	0.0	0.1	243	244	0.0	0.0	0.0	0.1
1.20	1000	1.0	243	243	0.1	0.1	0.1	0.1	243	243	0.0	0.0	0.0	0.1	243	244	0.0	0.0	0.0	0.1
1.20	1000	1.5	247	247	0.9	0.9	0.8	1.2	245	244	0.8	0.8	0.8	1.1	232	233	0.6	0.6	0.6	0.9
1.20	1000	2.0	246	246	2.1	2.1	2.1	3.2	243	243	2.0	2.0	2.0	3.1	235	235	1.7	1.7	1.7	2.6
1.20	1000	3.0	246	245	4.9	4.9	4.9	7.7	244	243	4.8	4.8	4.8	7.3	235	236	4.2	4.2	4.2	6.3
1.20	1000	4.0	245	245	8.7	8.7	8.7	13.7	244	243	8.5	8.5	8.5	13.0	235	236	7.4	7.4	7.4	11.2
1.20	2000	0.5	487	486	0.1	0.1	0.1	0.2	486	487	0.1	0.1	0.1	0.2	486	486	0.1	0.1	0.1	0.1
1.20	2000	1.0	487	486	0.1	0.1	0.1	0.2	486	487	0.1	0.1	0.1	0.2	486	486	0.1	0.1	0.1	0.1
1.20	2000	1.5	495	495	1.7	1.7	1.6	2.4	489	489	1.6	1.6	1.5	2.3	465	466	1.3	1.3	1.2	1.8
1.20	2000	2.0	490	490	4.1	4.1	4.1	6.5	486	485	4.0	4.0	4.0	6.1	471	471	3.5	3.5	3.5	5.2
1.20	2000	3.0	490	490	9.8	9.8	9.8	15.4	486	486	9.5	9.5	9.5	14.7	471	472	8.3	8.3	8.3	12.6
1.20	2000	4.0	491	491	17.4	17.4	17.4	27.4	486	487	16.9	16.9	16.9	26.1	472	472	14.8	14.8	14.8	22.4

Table 3. Response of rigid hoseline to steady currents (Do = 9.5 inches, Di = 8.0 inches, Wet = 5 lb/ft, C_D = 0.75, C_L = 0.6, C_f = 0.3)

RIGID

S/L	Length (feet)	V (kts)	0 degree						15 degrees						30 degrees					
			max. defl. (feet)		axial ten. (Kips)		anchor load (Kips)		max. defl. (feet)		axial ten. (Kips)		anchor load (Kips)		max. defl. (feet)		axial ten. (Kips)		anchor load (Kips)	
			(1)	(2)	(1)	(2)	(1)	(2)	(1)	(2)	(1)	(2)	(1)	(2)	(1)	(2)	(1)	(2)	(1)	(2)
1.05	200	0.5	25	25	0.0	0.0	0.0	0.0	26	26	0.0	0.0	0.0	0.0	26	27	0.0	0.0	0.0	0.0
1.05	200	1.0	27	27	0.1	0.1	0.1	0.1	26	27	0.1	0.1	0.1	0.1	26	27	0.0	0.0	0.0	0.0
1.05	200	1.5	27	27	0.6	0.6	0.6	0.6	26	26	0.5	0.5	0.5	0.5	26	26	0.4	0.4	0.4	0.4
1.05	200	2.0	27	27	1.2	1.2	1.2	1.2	26	26	1.1	1.1	1.1	1.1	27	26	0.9	0.9	0.9	0.9
1.05	200	3.0	27	27	2.7	2.7	2.7	2.7	26	26	2.5	2.5	2.5	2.5	27	26	2.1	2.1	2.1	2.1
1.05	200	4.0	27	27	4.7	4.8	4.7	4.7	26	26	4.5	4.5	4.5	4.5	27	26	3.7	3.7	3.7	3.7
1.05	500	0.5	65	65	0.1	0.1	0.1	0.1	66	65	0.0	0.0	0.0	0.0	66	65	0.0	0.0	0.0	0.0
1.05	500	1.0	67	67	0.3	0.3	0.3	0.2	66	66	0.3	0.3	0.2	0.2	66	65	0.0	0.0	0.0	0.0
1.05	500	1.5	66	66	1.4	1.4	1.4	1.4	66	66	1.3	1.3	1.3	1.3	65	66	1.1	1.1	1.1	1.0
1.05	500	2.0	66	66	3.0	3.0	3.0	3.0	66	66	2.8	2.8	2.8	2.8	66	66	2.3	2.3	2.3	2.3
1.05	500	3.0	66	66	6.7	6.7	6.7	6.7	66	67	6.3	6.3	6.3	6.3	66	66	5.3	5.3	5.3	5.2
1.05	500	4.0	66	66	11.8	11.9	11.8	11.8	66	67	11.2	11.2	11.2	11.1	66	66	9.3	9.3	9.3	9.2
1.05	1000	0.5	132	132	0.1	0.1	0.1	0.1	132	132	0.1	0.1	0.1	0.1	132	132	0.1	0.1	0.1	0.1
1.05	1000	1.0	133	133	0.7	0.7	0.5	0.5	131	132	0.6	0.6	0.5	0.4	132	132	0.1	0.1	0.1	0.1
1.05	1000	1.5	133	133	2.9	2.9	2.8	2.8	132	133	2.7	2.7	2.7	2.6	131	131	2.1	2.1	2.1	2.1
1.05	1000	2.0	133	133	5.9	5.9	5.9	5.9	133	133	5.6	5.6	5.6	5.6	132	131	4.7	4.7	4.7	4.6
1.05	1000	3.0	133	133	13.3	13.3	13.3	13.3	134	133	12.6	12.6	12.6	12.5	132	132	10.5	10.5	10.5	10.4
1.05	1000	4.0	134	134	23.6	23.6	23.6	23.7	134	133	22.3	22.4	22.4	22.3	132	133	18.6	18.6	18.6	18.5
1.05	2000	0.5	265	265	0.2	0.2	0.2	0.2	265	264	0.2	0.2	0.2	0.2	265	265	0.2	0.2	0.2	0.2
1.05	2000	1.0	268	268	1.3	1.3	1.0	1.0	264	264	1.2	1.2	0.9	0.8	265	265	0.2	0.2	0.2	0.2
1.05	2000	1.5	267	267	5.8	5.8	5.6	5.6	266	266	5.3	5.3	5.3	5.2	262	262	4.2	4.2	4.2	4.2
1.05	2000	2.0	267	267	11.8	11.9	11.8	11.8	268	267	11.2	11.2	11.2	11.1	264	264	9.3	9.3	9.3	9.2
1.05	2000	3.0	269	269	26.5	26.5	26.5	26.6	269	269	25.1	25.2	25.1	25.1	265	265	20.9	21.0	21.0	20.8
1.05	2000	4.0	271	271	46.8	46.9	46.8	47.3	271	270	44.4	44.5	44.4	44.5	267	267	37.0	37.1	37.1	36.9
1.10	200	0.5	36	36	0.0	0.0	0.0	0.0	36	36	0.0	0.0	0.0	0.0	36	36	0.0	0.0	0.0	0.0
1.10	200	1.0	37	37	0.1	0.1	0.1	0.1	37	37	0.1	0.1	0.0	0.1	36	36	0.0	0.0	0.0	0.0
1.10	200	1.5	36	36	0.4	0.4	0.4	0.5	36	36	0.4	0.4	0.4	0.5	35	35	0.3	0.3	0.3	0.4
1.10	200	2.0	36	36	0.8	0.8	0.8	1.1	35	36	0.8	0.8	0.8	1.0	35	36	0.7	0.7	0.7	0.8
1.10	200	3.0	36	36	1.8	1.8	1.8	2.4	35	36	1.8	1.8	1.8	2.2	35	36	1.5	1.5	1.5	1.9
1.10	200	4.0	36	36	3.3	3.3	3.3	4.2	35	36	3.1	3.1	3.1	4.0	35	36	2.7	2.7	2.7	3.4
1.10	500	0.5	91	91	0.0	0.0	0.0	0.1	91	91	0.0	0.0	0.0	0.0	91	91	0.0	0.0	0.0	0.0
1.10	500	1.0	93	93	0.2	0.2	0.1	0.2	92	92	0.2	0.2	0.1	0.1	91	91	0.0	0.0	0.0	0.0
1.10	500	1.5	91	91	1.0	1.0	1.0	1.2	91	90	0.9	0.9	0.9	1.1	89	89	0.7	0.7	0.7	0.9
1.10	500	2.0	91	91	2.0	2.0	2.0	2.6	90	91	2.0	2.0	2.0	2.5	89	90	1.7	1.7	1.7	2.1
1.10	500	3.0	91	91	4.6	4.6	4.6	5.9	90	91	4.4	4.4	4.4	5.6	89	90	3.7	3.7	3.7	4.7
1.10	500	4.0	92	92	8.2	8.2	8.2	10.5	91	91	7.8	7.8	7.8	10.0	89	90	6.6	6.6	6.6	8.4
1.10	1000	0.5	182	182	0.1	0.1	0.1	0.1	182	182	0.1	0.1	0.1	0.1	182	182	0.1	0.1	0.1	0.1
1.10	1000	1.0	186	186	0.4	0.4	0.3	0.3	185	185	0.3	0.3	0.2	0.3	182	182	0.1	0.1	0.1	0.1
1.10	1000	1.5	183	183	1.9	1.9	1.9	2.4	182	182	1.8	1.8	1.8	2.3	177	178	1.5	1.5	1.5	1.8
1.10	1000	2.0	183	183	4.1	4.1	4.1	5.3	182	181	3.9	3.9	3.9	5.0	179	178	3.3	3.3	3.3	4.2
1.10	1000	3.0	183	183	9.2	9.2	9.2	11.9	182	182	8.8	8.8	8.8	11.2	179	178	7.5	7.5	7.5	9.4
1.10	1000	4.0	183	183	16.3	16.3	16.3	21.1	182	182	15.6	15.6	15.6	19.9	179	179	13.2	13.2	13.2	16.8
1.10	2000	0.5	364	364	0.2	0.2	0.2	0.2	363	364	0.2	0.2	0.2	0.2	364	363	0.1	0.1	0.1	0.2
1.10	2000	1.0	373	373	0.8	0.8	0.5	0.6	369	369	0.7	0.7	0.5	0.5	364	363	0.1	0.1	0.1	0.2
1.10	2000	1.5	367	367	3.9	3.9	3.8	4.9	364	364	3.6	3.6	3.6	4.5	355	355	3.0	3.0	3.0	3.7
1.10	2000	2.0	366	366	8.2	8.2	8.2	10.5	364	365	7.8	7.8	7.8	10.0	358	358	6.6	6.6	6.6	8.4
1.10	2000	3.0	368	368	18.3	18.3	18.3	23.7	366	365	17.6	17.6	17.6	22.4	358	359	14.9	14.9	14.9	18.9
1.10	2000	4.0	368	368	32.5	32.5	32.5	42.1	367	366	31.1	31.2	31.1	39.8	360	359	26.4	26.4	26.4	33.6

RIGID

Table 3. Continued

S/L	Length (feet)	V (kts)	0 degree						15 degrees						30 degrees					
			max. defl. (feet)		axial ten. (Kips)		anchor load (Kips)		max. defl. (feet)		axial ten. (Kips)		anchor load (Kips)		max. defl. (feet)		axial ten. (Kips)		anchor load (Kips)	
			(1)	(2)	(1)	(2)	(1)	(2)	(1)	(2)	(1)	(2)	(1)	(2)	(1)	(2)	(1)	(2)	(1)	(2)
1.15	200	0.5	43	43	0.0	0.0	0.0	0.0	42	43	0.0	0.0	0.0	0.0	43	43	0.0	0.0	0.0	0.0
1.15	200	1.0	44	44	0.1	0.1	0.0	0.0	42	42	0.3	0.3	0.3	0.4	43	43	0.0	0.0	0.0	0.0
1.15	200	1.5	44	44	0.3	0.3	0.3	0.4	42	42	0.3	0.3	0.3	0.4	42	42	0.2	0.2	0.2	0.3
1.15	200	2.0	42	43	0.7	0.7	0.7	1.0	43	43	0.6	0.6	0.6	0.9	43	43	0.5	0.5	0.5	0.8
1.15	200	3.0	42	43	1.5	1.5	1.5	2.1	43	43	1.4	1.4	1.4	2.0	43	43	1.2	1.2	1.2	1.7
1.15	200	4.0	44	44	2.6	2.6	2.6	3.8	43	43	2.5	2.5	2.5	3.6	43	43	2.2	2.2	2.2	3.1
1.15	500	0.5	108	108	0.0	0.0	0.0	0.1	108	108	0.0	0.0	0.0	0.0	108	108	0.0	0.0	0.0	0.0
1.15	500	1.0	112	112	0.1	0.1	0.1	0.1	108	108	0.7	0.7	0.7	1.0	108	108	0.0	0.0	0.0	0.0
1.15	500	1.5	109	109	0.8	0.8	0.7	1.1	108	108	0.7	0.7	0.7	1.0	104	105	0.6	0.6	0.6	0.8
1.15	500	2.0	109	109	1.6	1.6	1.6	2.4	108	108	1.6	1.6	1.6	2.3	105	106	1.4	1.4	1.4	1.9
1.15	500	3.0	109	109	3.7	3.7	3.7	5.4	108	108	3.5	3.5	3.5	5.1	105	106	2.0	3.0	3.0	4.3
1.15	500	4.0	109	109	6.5	6.5	6.5	9.5	108	108	6.3	6.3	6.3	9.0	105	106	5.4	5.4	5.4	7.7
1.15	1000	0.5	216	216	0.1	0.1	0.1	0.1	216	216	0.1	0.1	0.1	0.1	217	216	0.1	0.1	0.1	0.1
1.15	1000	1.0	223	223	0.3	0.3	0.2	0.2	217	216	1.4	1.4	1.4	2.0	217	216	0.1	0.1	0.1	0.1
1.15	1000	1.5	218	218	1.5	1.5	1.5	2.1	217	216	1.4	1.4	1.4	2.0	210	210	1.2	1.2	1.2	1.6
1.15	1000	2.0	217	217	3.3	3.3	3.3	4.8	216	216	3.1	3.1	3.1	4.5	211	211	2.7	2.7	2.7	3.8
1.15	1000	3.0	218	218	7.3	7.3	7.3	10.7	216	216	7.1	7.1	7.1	10.2	211	211	6.1	6.1	6.1	8.6
1.15	1000	4.0	218	218	13.0	13.0	13.0	19.0	217	217	12.6	12.6	12.6	18.0	212	211	10.8	10.8	10.8	15.4
1.15	2000	0.5	432	432	0.1	0.1	0.1	0.2	433	433	0.1	0.1	0.1	0.2	433	433	0.1	0.1	0.1	0.2
1.15	2000	1.0	447	447	0.6	0.6	0.3	0.4	433	433	2.9	2.9	2.9	4.0	433	433	0.1	0.1	0.1	0.2
1.15	2000	1.5	437	437	3.0	3.0	3.0	4.3	433	433	2.9	2.9	2.9	4.0	420	419	2.4	2.4	2.4	3.3
1.15	2000	2.0	436	436	6.5	6.5	6.5	9.5	433	433	6.3	6.3	6.3	9.0	423	422	5.4	5.4	5.4	7.7
1.15	2000	3.0	437	437	14.6	14.6	14.6	21.4	433	434	14.1	14.1	14.1	20.3	423	423	12.2	12.2	12.2	17.3
1.15	2000	4.0	437	437	26.0	26.0	26.0	38.0	434	434	25.1	25.1	25.1	36.1	424	423	21.6	21.6	21.6	30.7
1.20	200	0.5	48	48	0.0	0.0	0.0	0.0	48	48	0.0	0.0	0.0	0.0	48	48	0.0	0.0	0.0	0.0
1.20	200	1.0	48	48	0.0	0.0	0.0	0.0	48	48	0.2	0.2	0.2	0.4	48	48	0.0	0.0	0.0	0.0
1.20	200	1.5	49	49	0.3	0.3	0.2	0.4	48	48	0.2	0.2	0.2	0.4	47	47	0.2	0.2	0.2	0.3
1.20	200	2.0	48	48	0.6	0.6	0.6	0.9	48	47	0.5	0.5	0.5	0.8	47	47	0.5	0.5	0.5	0.7
1.20	200	3.0	48	48	1.2	1.2	1.2	2.0	48	47	1.2	1.2	1.2	1.9	47	47	1.1	1.1	1.1	1.6
1.20	200	4.0	49	49	2.2	2.2	2.2	3.5	48	47	2.1	2.1	2.1	3.3	47	47	1.9	1.9	1.9	2.8
1.20	500	0.5	122	122	0.0	0.0	0.0	0.1	121	121	0.0	0.0	0.0	0.0	121	121	0.0	0.0	0.0	0.0
1.20	500	1.0	122	122	0.0	0.0	0.0	0.1	121	121	0.6	0.6	0.6	0.9	121	121	0.0	0.0	0.0	0.0
1.20	500	1.5	123	123	0.6	0.6	0.6	1.0	121	121	0.6	0.6	0.6	0.9	116	117	0.5	0.5	0.5	0.7
1.20	500	2.0	122	122	1.4	1.4	1.4	2.2	121	121	1.3	1.3	1.3	2.1	118	117	1.2	1.2	1.2	1.8
1.20	500	3.0	122	122	3.1	3.1	3.1	4.9	121	121	3.0	3.0	3.0	4.6	118	117	2.6	2.6	2.6	4.0
1.20	500	4.0	122	122	5.5	5.5	5.5	8.7	121	121	5.4	5.4	5.4	8.3	118	117	4.7	4.7	4.7	7.1
1.20	1000	0.5	243	243	0.1	0.1	0.1	0.1	243	243	0.1	0.1	0.1	0.1	243	244	0.0	0.0	0.1	0.1
1.20	1000	1.0	243	243	0.1	0.1	0.1	0.1	243	244	1.2	1.2	1.2	1.8	243	244	0.0	0.0	0.1	0.1
1.20	1000	1.5	246	246	1.3	1.3	1.2	1.9	243	244	1.2	1.2	1.2	1.8	234	233	1.0	1.0	1.0	1.5
1.20	1000	2.0	244	244	2.8	2.8	2.8	4.3	243	243	2.7	2.7	2.7	4.1	235	236	2.3	2.3	2.3	3.5
1.20	1000	3.0	246	245	6.2	6.2	6.2	9.8	244	243	6.0	6.0	6.0	9.3	235	236	5.3	5.3	5.3	8.0
1.20	1000	4.0	245	245	11.0	11.0	11.0	17.4	244	243	10.7	10.7	10.7	16.5	235	236	9.4	9.4	9.4	14.2
1.20	2000	0.5	487	486	0.1	0.1	0.1	0.2	487	487	0.1	0.1	0.1	0.2	486	486	0.1	0.1	0.1	0.2
1.20	2000	1.0	487	486	0.1	0.1	0.1	0.2	486	487	2.4	2.4	2.4	3.6	486	486	0.1	0.1	0.1	0.2
1.20	2000	1.5	492	493	2.5	2.5	2.5	3.8	486	487	2.4	2.4	2.4	3.6	467	467	2.0	2.0	2.0	2.9
1.20	2000	2.0	490	490	5.5	5.5	5.5	8.7	485	486	5.4	5.4	5.4	8.3	471	471	4.7	4.7	4.7	7.1
1.20	2000	3.0	490	490	12.4	12.4	12.4	19.6	486	486	12.1	12.1	12.1	18.6	471	472	10.5	10.5	10.5	15.9
1.20	2000	4.0	491	491	22.0	22.0	22.0	34.7	486	487	21.4	21.4	21.4	33.0	472	472	18.7	18.7	18.7	28.3

Table 4. Response of stretchable hoseline to steady currents (Do = 7.5 inches, Di = 6.0 inches, Wet = 5 lb/ft, C_D = 0.75, C_L = 0.6, C_f = 0.3)

STRETCHABLE

S/L	Length (feet)	V (kts)	0 degree						15 degrees						30 degrees					
			max. defl. (feet)		axial ten. (Kips)		anchor load (Kips)		max. defl. (feet)		axial ten. (Kips)		anchor load (Kips)		max. defl. (feet)		axial ten. (Kips)		anchor load (Kips)	
			(1)	(2)	(1)	(2)	(1)	(2)	(1)	(2)	(1)	(2)	(1)	(2)	(1)	(2)	(1)	(2)	(1)	(2)
1.05	200	0.5	25	25	0.0	0.0	0.0	0.0	26	26	0.0	0.0	0.0	0.0	26	27	0.0	0.0	0.0	0.0
1.05	200	1.0	25	25	0.0	0.0	0.0	0.0	26	26	0.0	0.0	0.0	0.0	26	27	0.0	0.0	0.0	0.0
1.05	200	1.5	28	28	0.4	0.4	0.4	0.4	28	28	0.4	0.4	0.3	0.4	28	27	0.3	0.3	0.3	0.3
1.05	200	2.0	30	30	0.8	0.8	0.8	0.9	29	30	0.8	0.8	0.8	0.8	29	30	0.6	0.6	0.6	0.7
1.05	200	3.0	34	34	1.7	1.7	1.7	2.0	33	33	1.6	1.6	1.6	1.9	32	32	1.4	1.4	1.4	1.6
1.05	200	4.0	37	37	2.7	2.7	2.7	3.5	37	37	2.6	2.6	2.6	3.3	35	35	2.3	2.3	2.3	2.8
1.05	500	0.5	65	65	0.0	0.0	0.0	0.0	66	65	0.0	0.0	0.0	0.0	66	65	0.0	0.0	0.0	0.0
1.05	500	1.0	65	65	0.0	0.0	0.0	0.0	66	65	0.0	0.0	0.0	0.0	66	65	0.0	0.0	0.0	0.0
1.05	500	1.5	77	77	0.9	0.9	0.9	0.9	75	75	0.8	0.8	0.8	0.9	72	73	0.7	0.7	0.6	0.7
1.05	500	2.0	85	85	1.8	1.8	1.8	2.2	84	85	1.7	1.7	1.7	2.0	81	80	1.5	1.5	1.5	1.7
1.05	500	3.0	102	102	3.6	3.6	3.6	4.8	100	100	3.5	3.5	3.5	4.6	94	93	3.1	3.1	3.1	3.9
1.05	500	4.0	118	118	5.7	5.7	5.7	8.2	115	116	5.5	5.5	5.5	7.9	107	108	4.9	4.9	4.9	6.8
1.05	1000	0.5	132	132	0.1	0.1	0.1	0.1	132	132	0.1	0.1	0.1	0.1	132	132	0.1	0.1	0.1	0.1
1.05	1000	1.0	132	132	0.1	0.1	0.1	0.1	132	132	0.1	0.1	0.1	0.1	132	132	0.1	0.1	0.1	0.1
1.05	1000	1.5	169	169	1.7	1.7	1.6	1.8	166	166	1.5	1.5	1.5	1.7	155	156	1.2	1.2	1.2	1.3
1.05	1000	2.0	198	198	3.2	3.2	3.2	4.2	194	194	3.1	3.1	3.1	4.0	182	182	2.7	2.7	2.7	3.3
1.05	1000	3.0	245	245	6.2	6.2	6.2	9.2	239	238	6.1	6.1	6.1	8.8	222	222	5.4	5.4	5.4	7.5
1.05	1000	4.0	292	292	9.7	9.7	9.7	15.5	283	283	9.5	9.5	9.5	14.8	260	260	8.6	8.6	8.6	12.9
1.05	2000	0.5	265	265	0.2	0.2	0.2	0.2	265	264	0.2	0.2	0.2	0.2	265	265	0.1	0.1	0.1	0.1
1.05	2000	1.0	265	265	0.2	0.2	0.2	0.2	265	264	0.2	0.2	0.2	0.2	265	265	0.1	0.1	0.1	0.1
1.05	2000	1.5	387	387	2.9	2.9	2.8	3.5	377	377	2.8	2.8	2.7	3.3	347	347	2.2	2.2	2.2	2.6
1.05	2000	2.0	471	472	5.6	5.6	5.6	8.1	460	460	5.4	5.4	5.4	7.7	428	427	4.8	4.8	4.8	6.6
1.05	2000	3.0	606	606	10.6	10.6	10.6	17.2	588	588	10.5	10.5	10.5	16.5	539	538	9.5	9.5	9.5	14.4
1.05	2000	4.0	705	705	17.0	17.0	17.0	29.1	684	683	16.9	16.9	16.9	27.9	629	629	15.4	15.4	15.4	24.5
1.10	200	0.5	36	36	0.0	0.0	0.0	0.0	36	36	0.0	0.0	0.0	0.0	36	36	0.0	0.0	0.0	0.0
1.10	200	1.0	36	36	0.0	0.0	0.0	0.0	36	36	0.0	0.0	0.0	0.0	36	36	0.0	0.0	0.0	0.0
1.10	200	1.5	37	37	0.3	0.3	0.3	0.3	37	37	0.2	0.2	0.2	0.3	36	36	0.2	0.2	0.2	0.2
1.10	200	2.0	38	38	0.6	0.6	0.6	0.8	38	38	0.6	0.6	0.6	0.7	37	37	0.5	0.5	0.5	0.6
1.10	200	3.0	40	40	1.3	1.3	1.3	1.8	40	40	1.3	1.3	1.3	1.7	39	40	1.1	1.1	1.1	1.5
1.10	200	4.0	44	44	2.2	2.2	2.2	3.2	43	43	2.1	2.1	2.1	3.0	42	41	1.9	1.9	1.9	2.6
1.10	500	0.5	91	91	0.0	0.0	0.0	0.0	91	91	0.0	0.0	0.0	0.0	91	91	0.0	0.0	0.0	0.0
1.10	500	1.0	91	91	0.0	0.0	0.0	0.0	91	91	0.0	0.0	0.0	0.0	91	91	0.0	0.0	0.0	0.0
1.10	500	1.5	97	97	0.7	0.7	0.6	0.8	95	96	0.6	0.6	0.6	0.7	92	91	0.5	0.5	0.5	0.6
1.10	500	2.0	104	104	1.4	1.4	1.4	1.9	103	102	1.3	1.3	1.3	1.8	98	99	1.2	1.2	1.2	1.5
1.10	500	3.0	115	115	3.0	3.0	3.0	4.4	113	114	2.9	2.9	2.9	4.2	108	107	2.6	2.6	2.6	3.6
1.10	500	4.0	129	129	4.9	4.9	4.9	7.6	126	125	4.8	4.8	4.8	7.2	118	118	4.3	4.3	4.3	6.2
1.10	1000	0.5	182	182	0.1	0.1	0.1	0.1	182	182	0.1	0.1	0.1	0.1	182	182	0.0	0.0	0.0	0.1
1.10	1000	1.0	182	182	0.1	0.1	0.1	0.1	182	182	0.1	0.1	0.1	0.1	182	182	0.0	0.0	0.0	0.1
1.10	1000	1.5	204	204	1.2	1.2	1.2	1.6	202	201	1.2	1.2	1.1	1.5	190	190	0.9	0.9	0.9	1.2
1.10	1000	2.0	226	226	2.6	2.6	2.6	3.8	222	222	2.5	2.5	2.5	3.6	211	211	2.2	2.2	2.2	3.1
1.10	1000	3.0	264	264	5.4	5.4	5.4	8.4	259	259	5.3	5.3	5.3	8.1	242	241	4.7	4.7	4.7	7.0
1.10	1000	4.0	305	305	8.6	8.6	8.6	14.3	297	297	8.5	8.5	8.5	13.7	275	275	7.7	7.7	7.7	12.0
1.10	2000	0.5	364	364	0.1	0.1	0.1	0.2	363	364	0.1	0.1	0.1	0.2	364	363	0.1	0.1	0.1	0.1
1.10	2000	1.0	364	364	0.1	0.1	0.1	0.2	363	364	0.1	0.1	0.1	0.2	364	363	0.1	0.1	0.1	0.1
1.10	2000	1.5	444	444	2.3	2.3	2.2	3.1	436	435	2.2	2.2	2.1	2.9	405	404	1.8	1.8	1.7	2.3
1.10	2000	2.0	514	514	4.8	4.8	4.8	7.4	503	502	4.7	4.7	4.7	7.0	470	470	4.1	4.1	4.1	6.0
1.10	2000	3.0	633	633	9.5	9.5	9.5	16.0	613	615	9.4	9.4	9.4	15.3	566	566	8.6	8.6	8.6	13.4
1.10	2000	4.0	729	729	15.5	15.5	15.5	27.1	705	706	15.4	15.4	15.4	26.0	656	656	14.1	14.1	14.1	22.8

Table 4. Continued

STRETCHABLE

S/L	Length (feet)	V (kts)	0 degree						15 degrees						30 degrees					
			max. defl. (feet)		axial ten. (Kips)		anchor load (Kips)		max. defl. (feet)		axial ten. (Kips)		anchor load (Kips)		max. defl. (feet)		axial ten. (Kips)		anchor load (Kips)	
			(1)	(2)	(1)	(2)	(1)	(2)	(1)	(2)	(1)	(2)	(1)	(2)	(1)	(2)	(1)	(2)	(1)	(2)
1.15	200	0.5	43	43	0.0	0.0	0.0	0.0	42	43	0.0	0.0	0.0	0.0	43	43	0.0	0.0	0.0	0.0
1.15	200	1.0	43	43	0.0	0.0	0.0	0.0	42	43	0.0	0.0	0.0	0.0	43	43	0.0	0.0	0.0	0.0
1.15	200	1.5	44	44	0.2	0.2	0.2	0.3	43	43	0.2	0.2	0.2	0.3	42	42	0.2	0.2	0.1	0.2
1.15	200	2.0	45	45	0.5	0.5	0.5	0.7	44	44	0.5	0.5	0.5	0.7	44	43	0.4	0.4	0.4	0.6
1.15	200	3.0	46	46	1.1	1.1	1.1	1.7	45	45	1.1	1.1	1.1	1.6	44	45	0.9	0.9	0.9	1.3
1.15	200	4.0	49	49	1.9	1.9	1.9	2.9	48	48	1.8	1.8	1.8	2.8	46	46	1.6	1.6	1.6	2.4
1.15	500	0.5	108	108	0.0	0.0	0.0	0.0	108	108	0.0	0.0	0.0	0.0	108	108	0.0	0.0	0.0	0.0
1.15	500	1.0	108	108	0.0	0.0	0.0	0.0	108	108	0.0	0.0	0.0	0.0	108	108	0.0	0.0	0.0	0.0
1.15	500	1.5	113	113	0.5	0.5	0.5	0.7	112	112	0.5	0.5	0.5	0.6	106	106	0.4	0.4	0.4	0.5
1.15	500	2.0	118	118	1.2	1.2	1.2	1.7	116	116	1.1	1.1	1.1	1.7	112	111	1.0	1.0	1.0	1.4
1.15	500	3.0	127	127	2.6	2.6	2.6	4.0	125	124	2.5	2.5	2.5	3.8	119	119	2.2	2.2	2.2	3.3
1.15	500	4.0	138	138	4.3	4.3	4.3	7.0	135	135	4.2	4.2	4.2	6.7	128	128	3.8	3.8	3.8	5.8
1.15	1000	0.5	216	216	0.1	0.1	0.1	0.1	216	216	0.1	0.1	0.1	0.1	217	216	0.0	0.0	0.0	0.1
1.15	1000	1.0	216	216	0.1	0.1	0.1	0.1	216	216	0.1	0.1	0.1	0.1	217	216	0.0	0.0	0.0	0.1
1.15	1000	1.5	234	235	1.0	1.0	0.9	1.4	231	231	0.9	0.9	0.9	1.3	217	216	0.7	0.7	0.7	1.0
1.15	1000	2.0	249	249	2.2	2.2	2.2	3.5	245	245	2.2	2.2	2.2	3.3	234	235	1.9	1.9	1.9	2.8
1.15	1000	3.0	283	283	4.8	4.8	4.8	7.8	276	276	4.7	4.7	4.7	7.4	260	260	4.2	4.2	4.2	6.5
1.15	1000	4.0	319	319	7.8	7.8	7.8	13.3	311	310	7.7	7.7	7.7	12.8	288	288	7.0	7.0	7.0	11.2
1.15	2000	0.5	432	432	0.1	0.1	0.1	0.2	433	433	0.1	0.1	0.1	0.2	433	433	0.1	0.1	0.1	0.1
1.15	2000	1.0	432	432	0.1	0.1	0.1	0.2	433	433	0.1	0.1	0.1	0.2	433	433	0.1	0.1	0.1	0.1
1.15	2000	1.5	495	495	1.9	1.9	1.8	2.7	485	485	1.8	1.8	1.7	2.5	452	453	1.4	1.4	1.4	2.0
1.15	2000	2.0	551	551	4.2	4.2	4.2	6.8	540	539	4.1	4.1	4.1	6.4	507	508	3.6	3.6	3.6	5.5
1.15	2000	3.0	657	656	8.6	8.6	8.6	14.9	638	637	8.6	8.6	8.6	14.2	590	591	7.8	7.8	7.8	12.5
1.15	2000	4.0	750	750	14.2	14.2	14.2	25.4	727	727	14.2	14.2	14.2	24.3	689	689	13.0	13.0	13.0	21.4
1.20	200	0.5	48	48	0.0	0.0	0.0	0.0	48	48	0.0	0.0	0.0	0.0	48	48	0.0	0.0	0.0	0.0
1.20	200	1.0	48	48	0.0	0.0	0.0	0.0	48	48	0.0	0.0	0.0	0.0	48	48	0.0	0.0	0.0	0.0
1.20	200	1.5	49	49	0.2	0.2	0.2	0.2	49	49	0.2	0.2	0.2	0.2	46	46	0.1	0.1	0.1	0.2
1.20	200	2.0	50	50	0.4	0.4	0.4	0.6	48	49	0.4	0.4	0.4	0.6	48	48	0.3	0.3	0.3	0.5
1.20	200	3.0	51	51	0.9	0.9	0.9	1.5	51	50	0.9	0.9	0.9	1.4	49	49	0.8	0.8	0.8	1.2
1.20	200	4.0	52	52	1.6	1.6	1.6	2.7	51	51	1.6	1.6	1.6	2.5	50	51	1.4	1.4	1.4	2.2
1.20	500	0.5	122	122	0.0	0.0	0.0	0.0	121	121	0.0	0.0	0.0	0.0	121	121	0.0	0.0	0.0	0.0
1.20	500	1.0	122	122	0.0	0.0	0.0	0.0	121	121	0.0	0.0	0.0	0.0	121	121	0.0	0.0	0.0	0.0
1.20	500	1.5	126	126	0.4	0.4	0.4	0.6	124	124	0.4	0.4	0.4	0.6	118	118	0.3	0.3	0.3	0.4
1.20	500	2.0	128	128	1.0	1.0	1.0	1.6	128	128	1.0	1.0	1.0	1.5	122	123	0.9	0.9	0.8	1.3
1.20	500	3.0	137	137	2.3	2.3	2.3	3.7	134	135	2.2	2.2	2.2	3.6	129	129	2.0	2.0	2.0	3.1
1.20	500	4.0	147	147	3.8	3.8	3.8	6.5	143	144	3.8	3.8	3.8	6.2	135	136	3.4	3.4	3.4	5.4
1.20	1000	0.5	243	243	0.1	0.1	0.1	0.1	243	243	0.0	0.0	0.0	0.1	243	244	0.0	0.0	0.0	0.1
1.20	1000	1.0	243	243	0.1	0.1	0.1	0.1	243	243	0.0	0.0	0.0	0.1	243	244	0.0	0.0	0.0	0.1
1.20	1000	1.5	259	259	0.8	0.8	0.8	1.2	254	255	0.8	0.8	0.8	1.1	240	241	0.6	0.6	0.6	0.9
1.20	1000	2.0	270	270	1.9	1.9	1.9	3.2	266	265	1.9	1.9	1.9	3.0	253	254	1.7	1.7	1.7	2.6
1.20	1000	3.0	299	299	4.3	4.3	4.3	7.2	292	292	4.2	4.2	4.2	6.9	275	275	3.8	3.8	3.8	6.0
1.20	1000	4.0	330	330	7.1	7.1	7.1	12.5	321	322	7.1	7.1	7.1	11.9	301	300	6.4	6.4	6.4	10.5
1.20	2000	0.5	487	486	0.1	0.1	0.1	0.2	486	487	0.1	0.1	0.1	0.2	486	486	0.1	0.1	0.1	0.1
1.20	2000	1.0	487	486	0.1	0.1	0.1	0.2	486	487	0.1	0.1	0.1	0.2	486	486	0.1	0.1	0.1	0.1
1.20	2000	1.5	538	538	1.6	1.6	1.5	2.4	528	528	1.5	1.5	1.5	2.2	495	496	1.2	1.2	1.2	1.7
1.20	2000	2.0	585	585	3.7	3.7	3.7	6.2	572	572	3.7	3.7	3.7	5.9	540	540	3.3	3.3	3.3	5.1
1.20	2000	3.0	678	678	7.9	7.9	7.9	13.9	658	660	7.9	7.9	7.9	13.3	617	617	7.2	7.2	7.2	11.7
1.20	2000	4.0	770	771	13.1	13.1	13.1	23.8	744	744	13.1	13.1	13.1	22.9	729	730	12.1	12.1	12.1	20.2

Table 5. Response of stretchable hoseline to steady currents (Do = 9.5 inches, Di = 8.0 inches, Wet = 5 lb/ft, C_D = 0.75, C_L = 0.6, C_f = 0.3)

STRETCHABLE

S/L	Length (feet)	V (kts)	0 degree						15 degrees						30 degrees					
			max. defl. (feet)		axial ten. (Kips)		anchor load (Kips)		max. defl. (feet)		axial ten. (Kips)		anchor load (Kips)		max. defl. (feet)		axial ten. (Kips)		anchor load (Kips)	
			(1)	(2)	(1)	(2)	(1)	(2)	(1)	(2)	(1)	(2)	(1)	(2)	(1)	(2)	(1)	(2)	(1)	(2)
1.05	200	0.5	25	25	0.0	0.0	0.0	0.0	26	26	0.0	0.0	0.0	0.0	26	27	0.0	0.0	0.0	0.0
1.05	200	1.0	28	28	0.3	0.3	0.3	0.3	27	28	0.3	0.3	0.2	0.2	26	27	0.2	0.2	0.2	0.2
1.05	200	1.5	30	30	0.8	0.8	0.8	0.9	29	30	0.8	0.8	0.8	0.9	29	30	0.6	0.6	0.6	0.7
1.05	200	2.0	33	33	1.4	1.4	1.4	1.7	33	32	1.4	1.4	1.4	1.6	31	31	1.2	1.2	1.2	1.3
1.05	200	3.0	38	38	2.8	2.8	2.8	3.6	38	37	2.7	2.7	2.7	3.4	36	36	2.3	2.3	2.3	2.9
1.05	200	4.0	44	44	4.5	4.5	4.5	6.2	42	42	4.3	4.3	4.3	5.9	40	40	3.7	3.7	3.7	5.0
1.05	500	0.5	65	65	0.1	0.1	0.1	0.1	66	65	0.1	0.1	0.1	0.1	66	65	0.1	0.1	0.1	0.1
1.05	500	1.0	74	74	0.7	0.7	0.6	0.6	73	73	0.6	0.6	0.6	0.6	69	69	0.4	0.4	0.4	0.4
1.05	500	1.5	86	86	1.8	1.8	1.8	2.2	85	85	1.7	1.7	1.7	2.1	81	80	1.5	1.5	1.5	1.7
1.05	500	2.0	98	98	3.1	3.1	3.1	4.0	96	96	2.9	2.9	2.9	3.8	91	90	2.5	2.5	2.5	3.2
1.05	500	3.0	119	119	5.8	5.8	5.8	8.5	117	117	5.6	5.6	5.6	8.1	109	108	4.9	4.9	4.9	6.9
1.05	500	4.0	142	142	9.0	9.0	9.0	14.3	138	138	8.7	8.7	8.7	13.6	127	127	7.7	7.7	7.7	11.8
1.05	1000	0.5	132	132	0.2	0.2	0.2	0.2	132	132	0.1	0.1	0.1	0.1	132	132	0.1	0.1	0.1	0.1
1.05	1000	1.0	160	160	1.2	1.2	1.1	1.2	157	157	1.1	1.1	1.0	1.1	146	146	0.8	0.8	0.7	0.8
1.05	1000	1.5	199	199	3.2	3.2	3.2	4.3	195	195	3.1	3.1	3.1	4.1	183	183	2.7	2.7	2.7	3.4
1.05	1000	2.0	232	232	5.3	5.3	5.3	7.6	227	227	5.1	5.1	5.1	7.3	211	210	4.5	4.5	4.5	6.2
1.05	1000	3.0	296	296	9.8	9.8	9.8	15.8	287	287	9.5	9.5	9.5	15.1	262	263	8.5	8.5	8.5	13.1
1.05	1000	4.0	344	344	15.6	15.6	15.6	26.6	334	335	15.2	15.2	15.2	25.4	308	308	13.5	13.5	13.5	22.0
1.05	2000	0.5	265	265	0.3	0.3	0.3	0.3	265	264	0.3	0.3	0.3	0.3	265	265	0.2	0.2	0.2	0.2
1.05	2000	1.0	360	360	2.2	2.2	2.0	2.4	350	350	2.1	2.1	1.8	2.2	317	318	1.6	1.6	1.4	1.6
1.05	2000	1.5	476	476	5.6	5.6	5.6	8.2	464	464	5.4	5.4	5.4	7.8	430	430	4.7	4.7	4.7	6.6
1.05	2000	2.0	570	570	9.0	9.0	9.0	14.3	554	554	8.7	8.7	8.7	13.6	508	508	7.7	7.7	7.7	11.8
1.05	2000	3.0	713	713	17.2	17.2	17.2	29.5	691	691	16.7	16.7	16.7	28.2	635	634	14.9	14.9	14.9	24.5
1.05	2000	4.0	822	821	27.8	27.8	27.8	49.6	796	796	27.1	27.1	27.1	47.4	753	752	24.1	24.1	24.1	41.2
1.10	200	0.5	36	36	0.0	0.0	0.0	0.0	36	36	0.0	0.0	0.0	0.0	36	36	0.0	0.0	0.0	0.0
1.10	200	1.0	37	37	0.2	0.2	0.2	0.2	37	37	0.2	0.2	0.2	0.2	34	35	0.1	0.1	0.1	0.1
1.10	200	1.5	38	38	0.6	0.6	0.6	0.8	38	38	0.6	0.6	0.6	0.8	37	37	0.5	0.5	0.5	0.6
1.10	200	2.0	41	41	1.1	1.1	1.1	1.5	39	39	1.0	1.0	1.0	1.4	38	38	0.9	0.9	0.9	1.2
1.10	200	3.0	44	44	2.3	2.3	2.3	3.3	43	43	2.2	2.2	2.2	3.1	42	41	1.9	1.9	1.9	2.6
1.10	200	4.0	48	48	3.8	3.8	3.8	5.7	48	48	3.6	3.6	3.6	5.4	45	45	3.1	3.1	3.1	4.6
1.10	500	0.5	91	91	0.1	0.1	0.1	0.1	91	91	0.1	0.1	0.1	0.1	91	91	0.0	0.0	0.0	0.1
1.10	500	1.0	96	96	0.5	0.5	0.4	0.5	94	95	0.4	0.4	0.4	0.5	89	88	0.3	0.3	0.3	0.3
1.10	500	1.5	104	104	1.4	1.4	1.4	2.0	103	102	1.4	1.4	1.4	1.9	98	99	1.1	1.1	1.1	1.5
1.10	500	2.0	112	112	2.5	2.5	2.5	3.6	111	110	2.4	2.4	2.4	3.4	105	105	2.1	2.1	2.1	2.9
1.10	500	3.0	130	130	5.0	5.0	5.0	7.8	127	127	4.8	4.8	4.8	7.4	119	119	4.2	4.2	4.2	6.3
1.10	500	4.0	150	150	8.0	8.0	8.0	13.2	146	145	7.7	7.7	7.7	12.5	134	135	6.8	6.8	6.8	10.8
1.10	1000	0.5	182	182	0.1	0.1	0.1	0.2	182	182	0.1	0.1	0.1	0.1	182	182	0.1	0.1	0.1	0.1
1.10	1000	1.0	199	199	0.9	0.9	0.8	1.0	196	196	0.8	0.8	0.7	0.9	182	182	0.6	0.6	0.5	0.6
1.10	1000	1.5	226	226	2.6	2.6	2.6	3.9	223	222	2.5	2.5	2.5	3.6	211	212	2.2	2.2	2.2	3.1
1.10	1000	2.0	253	253	4.5	4.5	4.5	7.0	249	248	4.4	4.4	4.4	6.6	233	234	3.8	3.8	3.8	5.7
1.10	1000	3.0	310	310	8.8	8.8	8.8	14.6	300	300	8.5	8.5	8.5	14.0	277	278	7.5	7.5	7.5	12.1
1.10	1000	4.0	357	357	14.1	14.1	14.1	24.6	347	346	13.7	13.7	13.7	23.5	321	322	12.2	12.2	12.2	20.4
1.10	2000	0.5	364	364	0.2	0.2	0.2	0.3	363	364	0.2	0.2	0.2	0.3	364	363	0.2	0.2	0.2	0.2
1.10	2000	1.0	425	425	1.7	1.7	1.5	2.0	415	416	1.6	1.6	1.4	1.8	380	380	1.2	1.2	1.0	1.3
1.10	2000	1.5	517	517	4.8	4.8	4.8	7.4	505	505	4.6	4.6	4.6	7.1	472	471	4.0	4.0	4.0	6.0
1.10	2000	2.0	599	599	8.0	8.0	8.0	13.2	583	583	7.7	7.7	7.7	12.5	539	539	6.8	6.8	6.8	10.8
1.10	2000	3.0	735	735	15.5	15.5	15.5	27.3	712	712	15.2	15.2	15.2	26.1	660	661	13.5	13.5	13.5	22.7
1.10	2000	4.0	844	844	25.4	25.4	25.4	46.0	815	816	24.8	24.8	24.8	44.0	797	799	22.1	22.1	22.1	38.3

Table 5. Continued

STRETCHABLE

S/L	Length (feet)	V (kts)	0 degree						15 degrees						30 degrees					
			max. defl. (feet)		axial ten. (Kips)		anchor load (Kips)		max. defl. (feet)		axial ten. (Kips)		anchor load (Kips)		max. defl. (feet)		axial ten. (Kips)		anchor load (Kips)	
			(1)	(2)	(1)	(2)	(1)	(2)	(1)	(2)	(1)	(2)	(1)	(2)	(1)	(2)	(1)	(2)	(1)	(2)
1.15	200	0.5	43	43	0.0	0.0	0.0	0.0	42	43	0.0	0.0	0.0	0.0	43	43	0.0	0.0	0.0	0.0
1.15	200	1.0	44	44	0.1	0.1	0.1	0.2	43	43	0.1	0.1	0.1	0.2	41	40	0.1	0.1	0.1	0.1
1.15	200	1.5	45	45	0.5	0.5	0.5	0.7	44	44	0.5	0.5	0.5	0.7	44	43	0.4	0.4	0.4	0.6
1.15	200	2.0	46	46	0.9	0.9	0.9	1.4	46	46	0.9	0.9	0.9	1.3	44	44	0.7	0.7	0.7	1.1
1.15	200	3.0	49	49	1.9	1.9	1.9	3.0	48	48	1.9	1.9	1.9	2.8	47	46	1.6	1.6	1.6	2.4
1.15	200	4.0	52	52	3.2	3.2	3.2	5.2	51	52	3.1	3.1	3.1	4.9	49	49	2.7	2.7	2.7	4.2
1.15	500	0.5	108	108	0.1	0.1	0.1	0.1	108	108	0.0	0.0	0.0	0.1	108	108	0.0	0.0	0.0	0.1
1.15	500	1.0	112	112	0.4	0.4	0.3	0.4	111	111	0.3	0.3	0.3	0.4	103	104	0.2	0.2	0.2	0.3
1.15	500	1.5	118	117	1.2	1.2	1.2	1.8	116	115	1.1	1.1	1.1	1.7	112	111	0.9	0.9	0.9	1.4
1.15	500	2.0	124	124	2.1	2.1	2.1	3.3	122	122	2.0	2.0	2.0	3.1	117	117	1.8	1.8	1.7	2.7
1.15	500	3.0	139	139	4.4	4.4	4.4	7.2	136	136	4.2	4.2	4.2	6.8	128	129	3.7	3.7	3.7	5.8
1.15	500	4.0	157	157	7.1	7.1	7.1	12.2	152	152	6.9	6.9	6.9	11.6	142	142	6.1	6.1	6.1	10.0
1.15	1000	0.5	216	216	0.1	0.1	0.1	0.2	216	216	0.1	0.1	0.1	0.1	217	216	0.1	0.1	0.1	0.1
1.15	1000	1.0	230	231	0.7	0.7	0.6	0.8	227	227	0.6	0.6	0.5	0.7	211	211	0.5	0.5	0.4	0.5
1.15	1000	1.5	250	251	2.2	2.2	2.2	3.5	246	246	2.1	2.1	2.1	3.3	234	235	1.8	1.8	1.8	2.8
1.15	1000	2.0	273	273	3.9	3.9	3.9	6.4	268	268	3.8	3.8	3.8	6.1	253	252	3.3	3.3	3.3	5.2
1.15	1000	3.0	322	322	7.9	7.9	7.9	13.5	312	314	7.7	7.7	7.7	12.9	290	290	6.8	6.8	6.8	11.2
1.15	1000	4.0	368	369	12.8	12.8	12.8	22.8	357	357	12.5	12.5	12.5	21.8	336	335	11.1	11.1	11.1	18.9
1.15	2000	0.5	432	432	0.2	0.2	0.2	0.3	433	433	0.2	0.2	0.2	0.3	433	433	0.2	0.2	0.2	0.2
1.15	2000	1.0	481	481	1.4	1.4	1.1	1.6	471	470	1.2	1.2	1.0	1.5	434	434	0.9	0.9	0.7	1.0
1.15	2000	1.5	554	554	4.2	4.2	4.2	6.8	543	543	4.0	4.0	4.0	6.4	509	508	3.5	3.5	3.5	5.4
1.15	2000	2.0	626	626	7.1	7.1	7.1	12.2	609	609	6.9	6.9	6.9	11.6	567	567	6.1	6.1	6.1	10.0
1.15	2000	3.0	755	755	14.2	14.2	14.2	25.4	732	731	13.9	13.9	13.9	24.3	692	693	12.3	12.3	12.3	21.1
1.15	2000	4.0	866	866	23.3	23.3	23.3	42.9	833	833	22.8	22.8	22.8	41.0	871	866	20.5	20.5	20.5	35.8
1.20	200	0.5	48	48	0.0	0.0	0.0	0.0	48	48	0.0	0.0	0.0	0.0	48	48	0.0	0.0	0.0	0.0
1.20	200	1.0	49	49	0.1	0.1	0.1	0.1	49	49	0.1	0.1	0.1	0.1	48	48	0.3	0.3	0.3	0.5
1.20	200	1.5	50	50	0.4	0.4	0.4	0.6	48	49	0.4	0.4	0.4	0.6	48	48	0.3	0.3	0.3	0.5
1.20	200	2.0	50	50	0.8	0.8	0.8	1.2	49	49	0.7	0.7	0.7	1.2	48	49	0.6	0.6	0.6	1.0
1.20	200	3.0	53	53	1.7	1.7	1.7	2.7	52	53	1.6	1.6	1.6	2.6	50	51	1.4	1.4	1.4	2.2
1.20	200	4.0	56	56	2.9	2.9	2.9	4.8	55	54	2.8	2.8	2.8	4.5	53	53	2.4	2.4	2.4	3.9
1.20	500	0.5	122	122	0.0	0.0	0.0	0.1	121	121	0.0	0.0	0.0	0.1	121	121	0.0	0.0	0.0	0.1
1.20	500	1.0	127	126	0.3	0.3	0.2	0.3	124	124	0.3	0.3	0.2	0.3	122	122	0.6	0.6	0.8	1.3
1.20	500	1.5	130	130	1.0	1.0	1.0	1.6	128	128	1.0	1.0	1.0	1.5	122	123	0.8	0.8	0.8	1.3
1.20	500	2.0	135	135	1.9	1.9	1.9	3.0	132	132	1.8	1.8	1.8	2.9	126	127	1.5	1.5	1.5	2.5
1.20	500	3.0	147	147	3.9	3.9	3.9	6.6	144	144	3.8	3.8	3.8	6.3	137	136	3.3	3.3	3.3	5.4
1.20	500	4.0	162	162	6.5	6.5	6.5	11.3	157	158	6.3	6.3	6.3	10.8	148	148	5.6	5.6	5.6	9.3
1.20	1000	0.5	243	243	0.1	0.1	0.1	0.2	243	243	0.1	0.1	0.1	0.1	243	244	0.1	0.1	0.1	0.1
1.20	1000	1.0	257	257	0.6	0.6	0.5	0.7	253	252	0.5	0.5	0.4	0.6	251	250	1.3	1.3	1.6	2.5
1.20	1000	1.5	272	271	1.9	1.9	1.9	3.2	266	266	1.9	1.9	1.9	3.0	254	254	1.6	1.6	1.6	2.5
1.20	1000	2.0	290	290	3.5	3.5	3.5	5.9	284	284	3.4	3.4	3.4	5.6	269	268	2.9	2.9	2.9	4.8
1.20	1000	3.0	332	333	7.2	7.2	7.2	12.6	323	323	7.0	7.0	7.0	12.0	303	303	6.2	6.2	6.2	10.4
1.20	1000	4.0	378	378	11.8	11.8	11.8	21.3	365	366	11.5	11.5	11.5	20.3	352	352	10.2	10.2	10.2	17.7
1.20	2000	0.5	487	486	0.2	0.2	0.2	0.3	487	487	0.2	0.2	0.2	0.3	486	486	0.1	0.1	0.1	0.2
1.20	2000	1.0	528	528	1.1	1.1	0.9	1.3	517	518	1.0	1.0	0.8	1.2	528	528	2.4	2.4	3.1	5.0
1.20	2000	1.5	587	587	3.7	3.7	3.7	6.2	574	574	3.6	3.6	3.6	5.9	540	540	3.1	3.1	3.1	5.0
1.20	2000	2.0	651	651	6.5	6.5	6.5	11.3	633	633	6.3	6.3	6.3	10.8	593	592	5.6	5.6	5.6	9.3
1.20	2000	3.0	775	775	13.1	13.1	13.1	23.7	748	748	12.8	12.8	12.8	22.7	734	735	11.4	11.4	11.4	19.7
1.20	2000	4.0	884	884	21.6	21.6	21.6	40.1	842	842	21.2	21.2	21.2	38.5	990	991	19.1	19.1	19.1	33.7

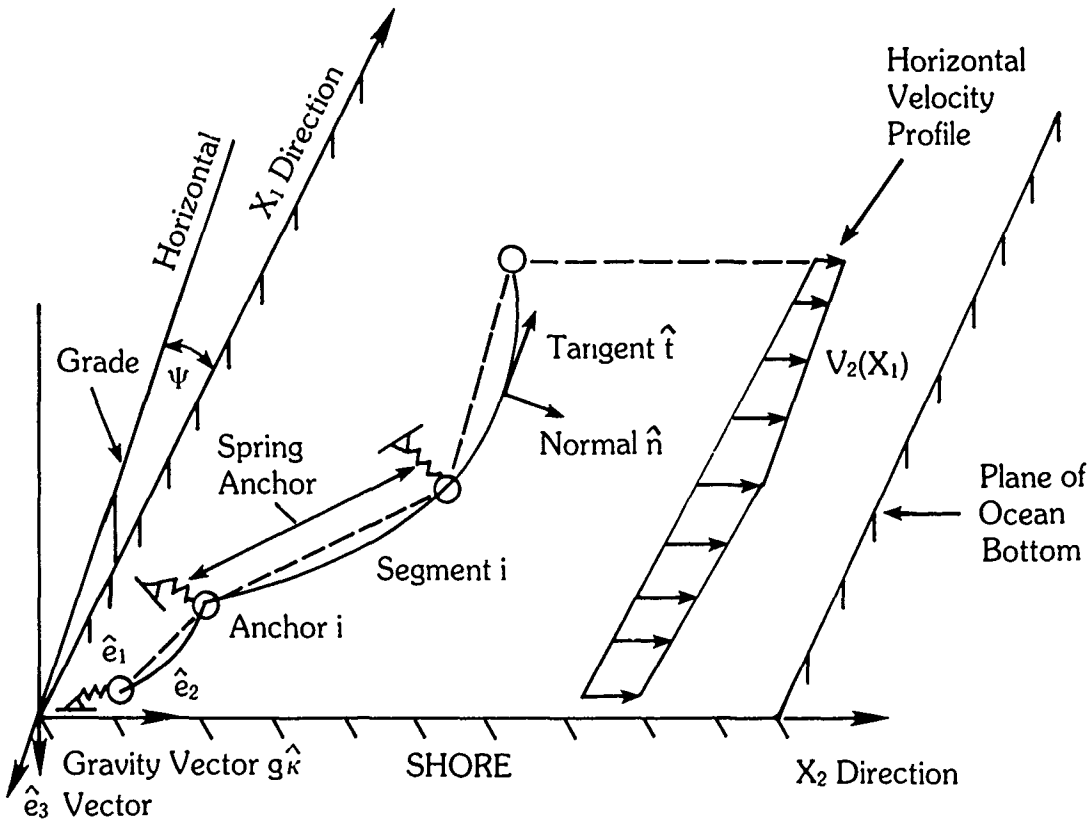

Figure 1. Definition sketch.

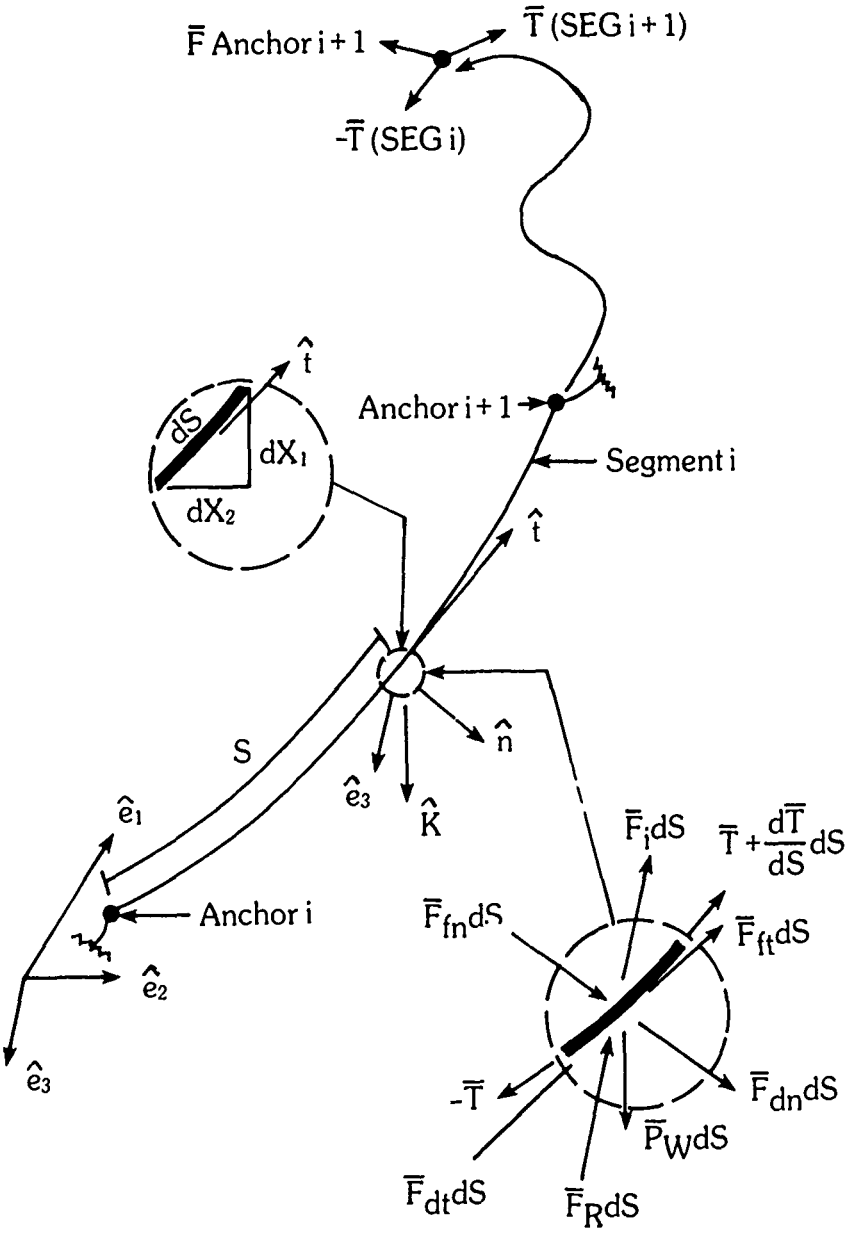

Figure 2. Vectors on a typical hose segment.

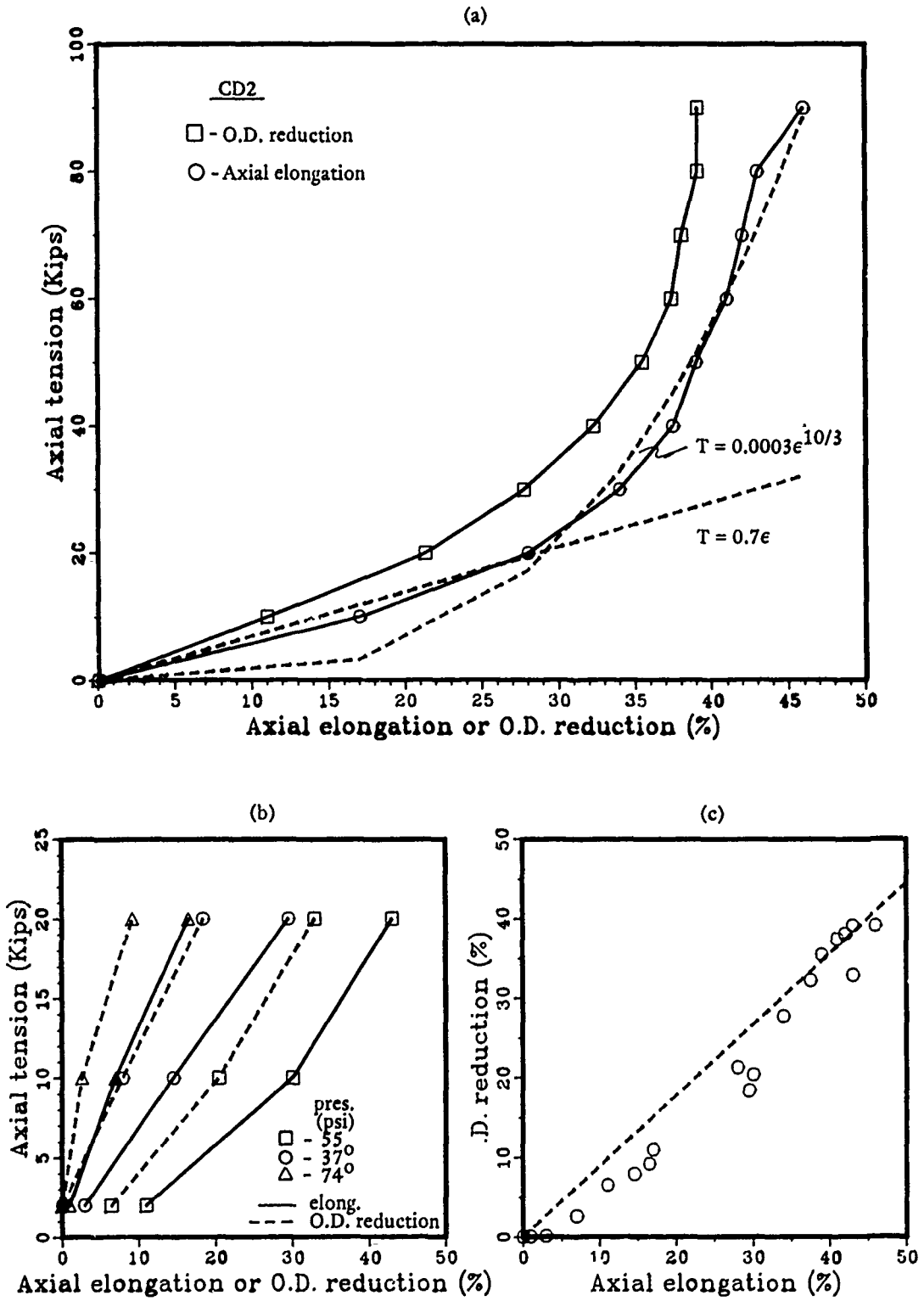

Figure 3. Behavior of a highly stretchable hose under axial tension.

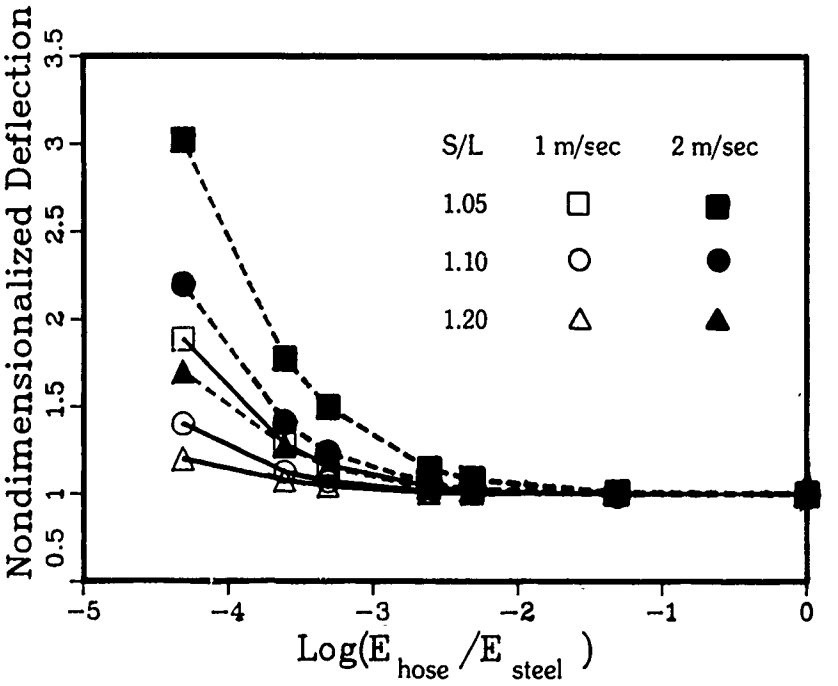

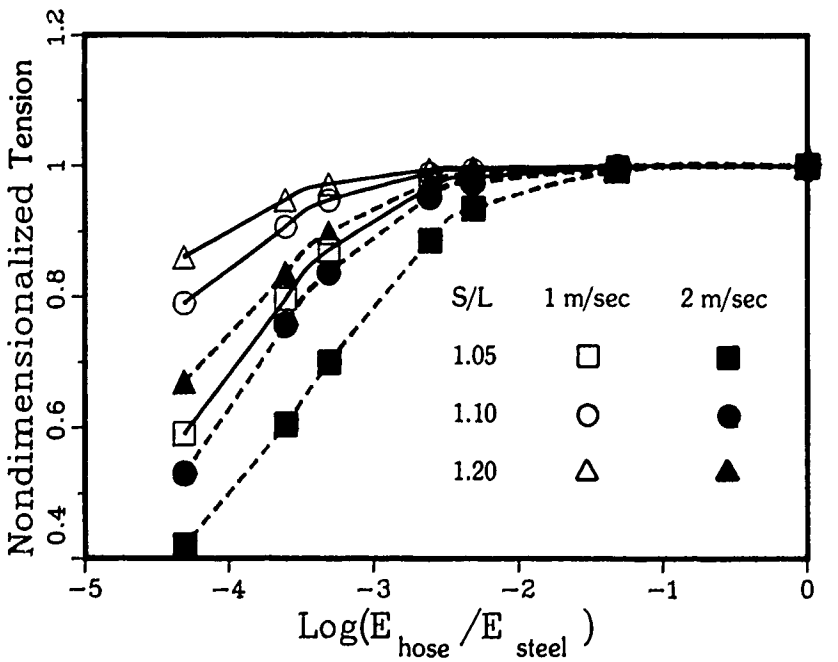

Figure 4. Influence of modulus of elasticity, E, on the response of a hoseline.

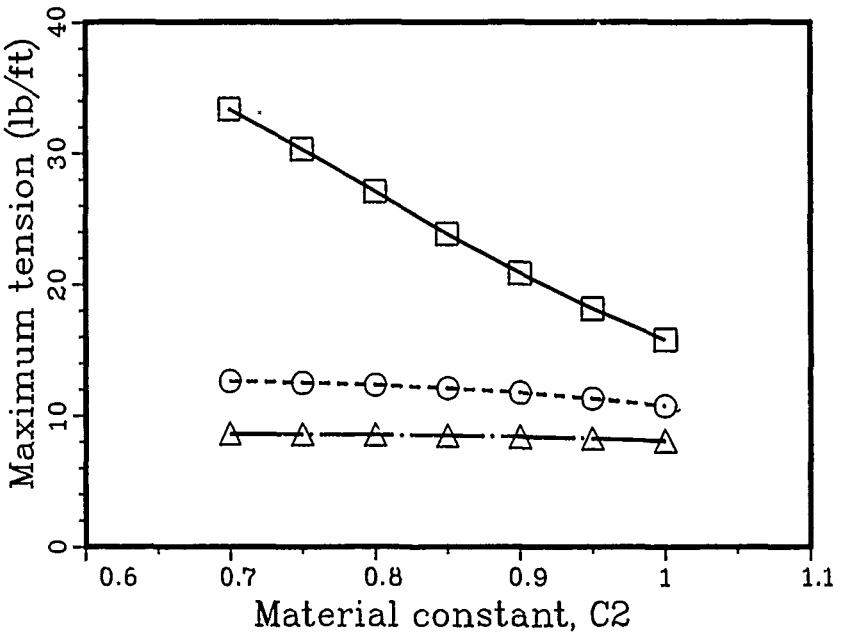

Figure 5. Influence of material constant C2 on the response of a hose in a 4-knot current.

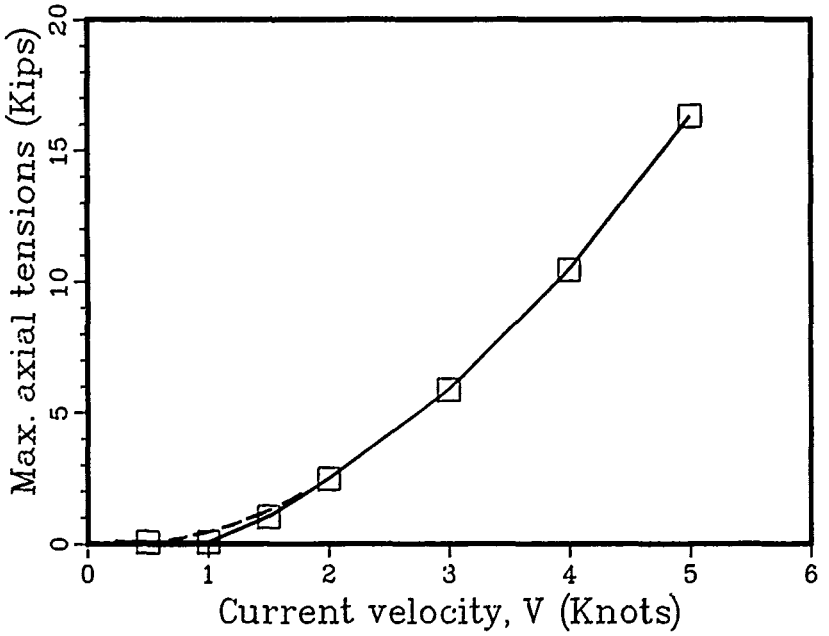

Figure 6. Influence of current velocity on the hose tension, S/L = 1.2.

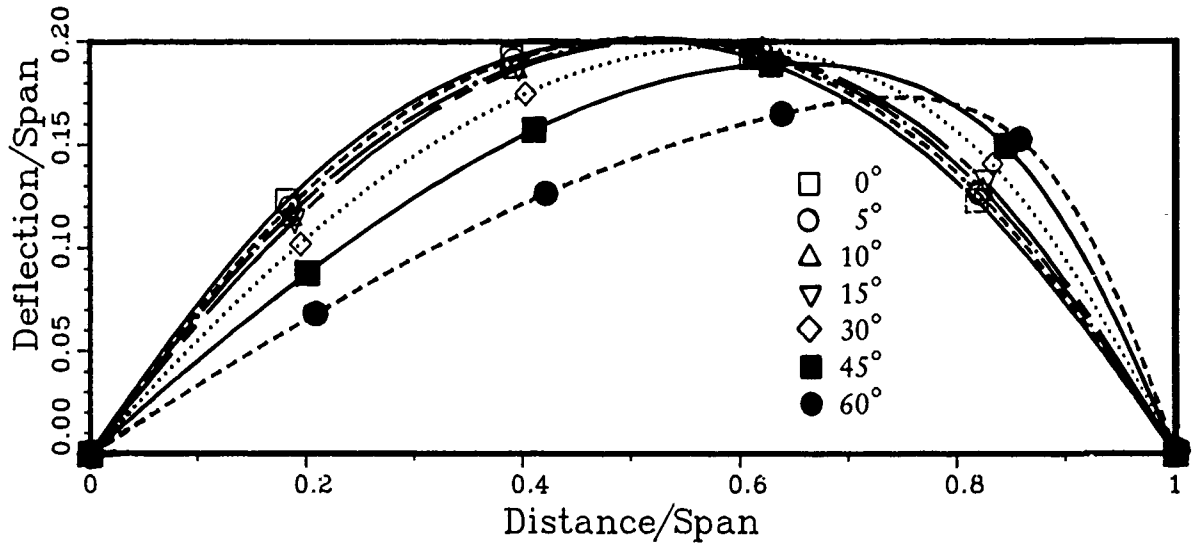

Figure 7. Geometry of the hose segment in currents of various directions.

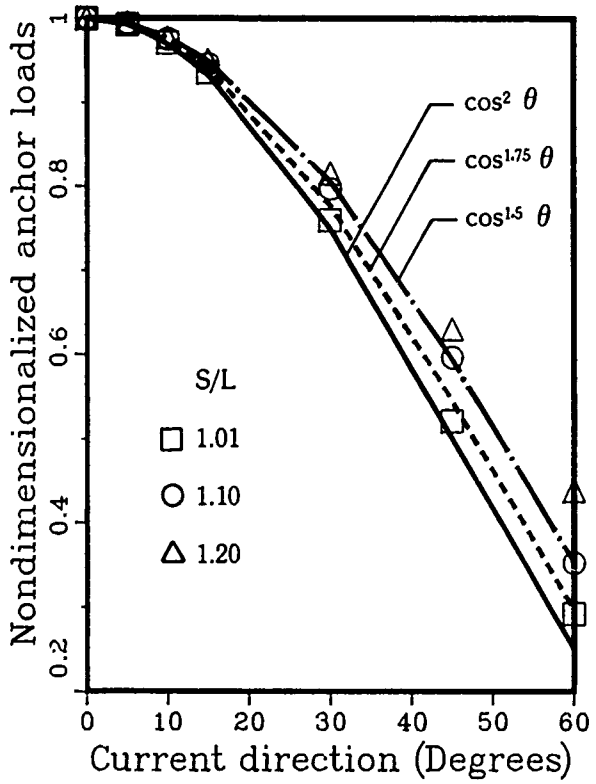

Figure 8. Influence of current direction on the anchor load, V = 4 knots.

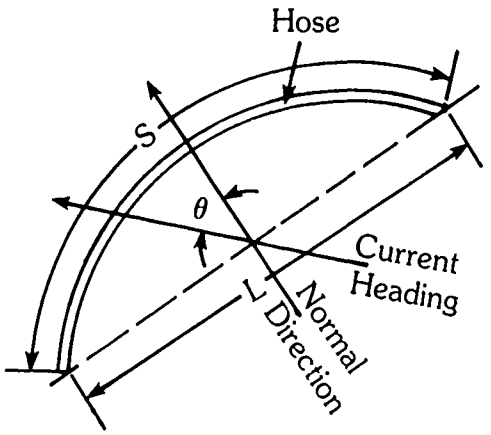

Figure 9. Definition of current direction.

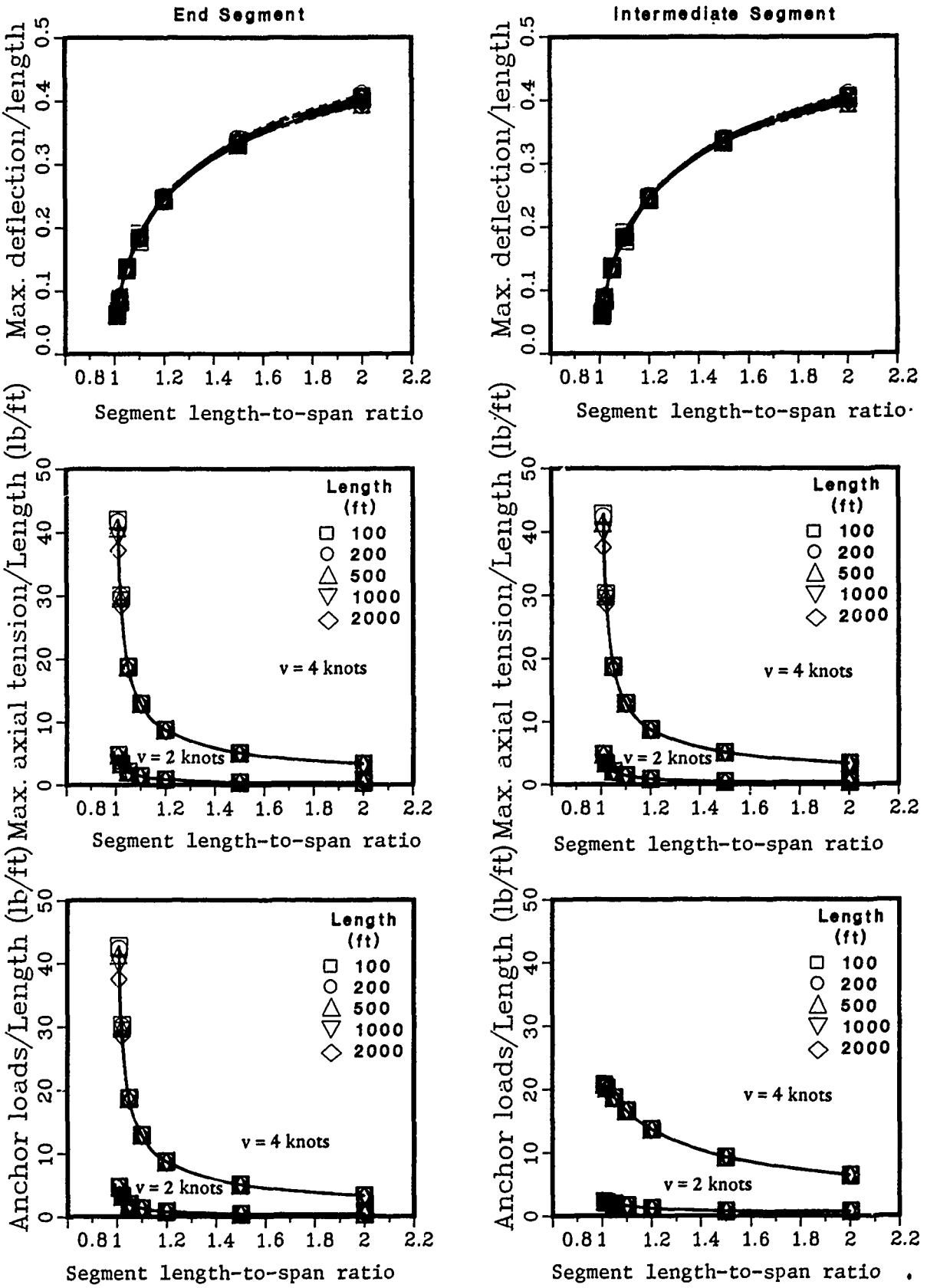

Figure 10. Influence of segment length-to-span ratio, S/L, on the response of a hoseline.

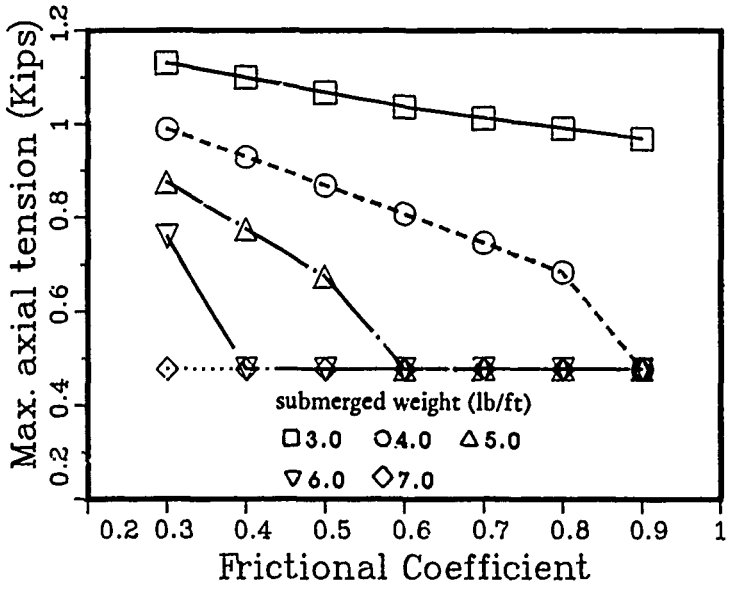

Figure 11. Influence of sea bottom friction on the hose tension in a 1.5-knot current. Segment length-to-span ratio, S/L = 1.2.

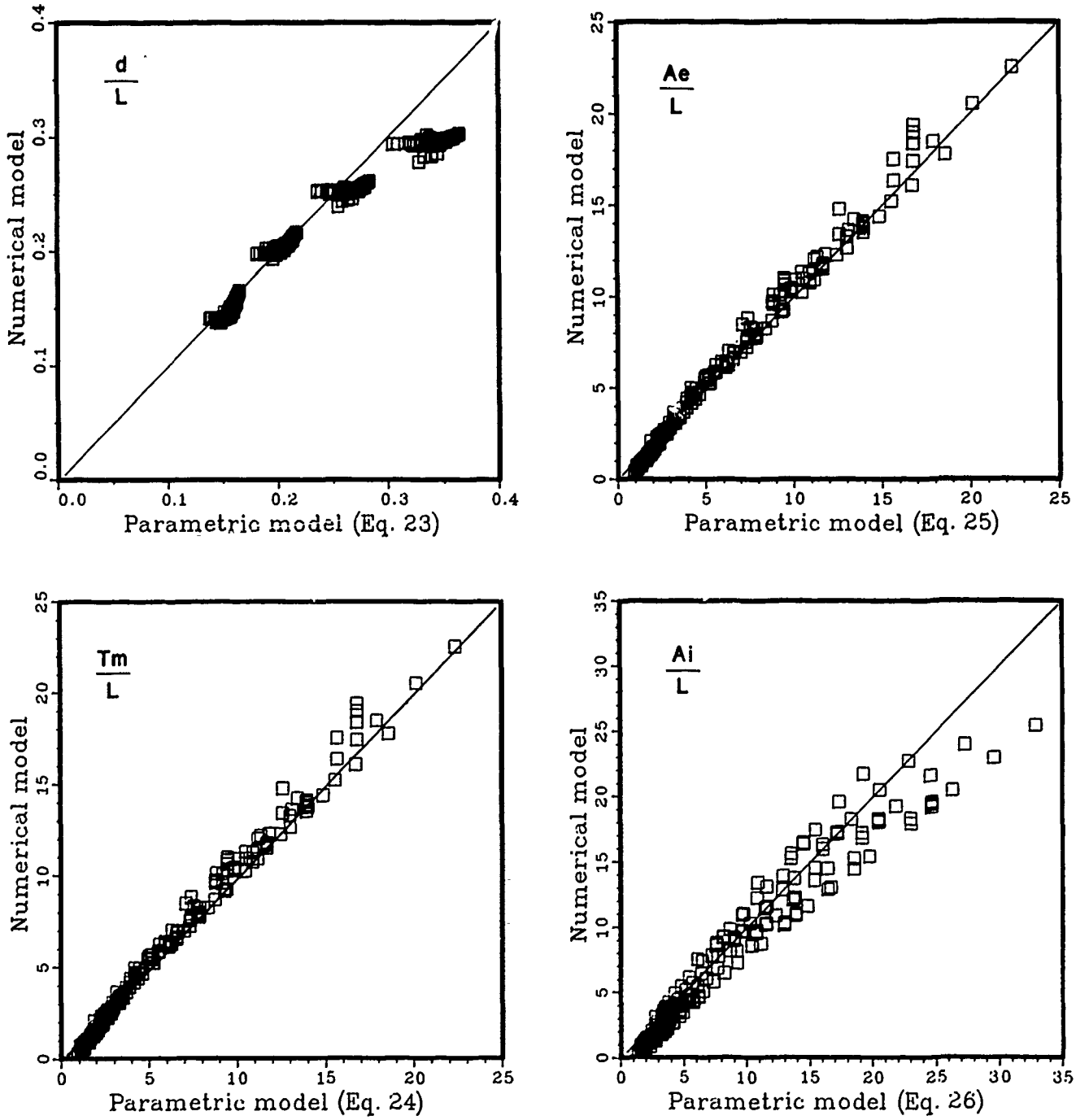

Figure 12. Parametric model versus numerical model.

Appendix A

NUMERICAL SOLUTION TECHNIQUES

A.1 NEWTON-RAPHSON QUASI-LINEARIZATION

Given a coupled set of nonlinear first-order differential equations, it is possible to develop a convergence acceleration procedure (Ref A-1) of successive iteration upon quasi-linear equations adopting methods proposed by Bellman (Ref A-2) and by Klaba (Ref A-3). Assume a set of 2N nonlinear first-order differential equations:

$$\frac{dy_i}{ds} = f_i(s,y_i) \qquad i,j = 1,2,\ldots,2N \tag{A.1.1}$$

with N boundary condition at the starting end s = 0

$$g_m(y_j^0) = 0 \qquad m = 1,2,\ldots,N \tag{A.1.2a}$$

and N boundary conditions at the terminating end S = 1,

$$h_m(y_j^1) = 0 \qquad m = 1,2,\ldots,N \tag{A.1.2b}$$

where S is the independent variable (e.g., hose arc length), y_i are the 2N dependent variables (e.g., tension components and location coordinates), $f_i(s,y_j)$ are nonlinear functions of y_j (e.g., hydrodynamic forcing functions), and $g_m(y_j^0)$ and $h_m(y_j^1)$ are nonlinear combinations of y_j^0 at s = 0, and of y_j^1 at s = 1, respectively.

Let y_j' denote a trial solution vector in the neighborhood of the true solution vector y_j. The $y_j^{0'}$ and $y_j^{1'}$ are corresponding boundary values of y_j' at s = 0 and s = 1, respectively. The nonlinear function $f_i(s,y_j)$, $g_m(y_j^0)$, and $f_m(y_j^1)$ can be written as truncated Taylor series expansions about y_j', $y_j^{0'}$ and $y_j^{1'}$ as:

$$f_i(s,y_j) = f_i(s,y'_j) + J_{ik}(y_k - y'_k) \qquad i,j,k = 1,2,\ldots,2N \qquad (A.1.3)$$

$$g_m(y^0_j) = g_m(y^{0,}_j) + J^0_{mk}(y^0_k - y^{0,}_k) \qquad m = 1,2,\ldots,N$$

$$h_m(y^1_j) = h_m(y^{1,}_j) + J^1_{mk}(y^1_k - y^{1,}_k) \qquad m - 1,2,\ldots,N$$

where the summation conversion from 1 to 2N on repeated indices has been adopted, J_{ik} is the square Jacobian matrix of order 2Nx2N for the gradient of the nonlinear forcing function:

$$J_{ik} = \left[\frac{\partial f_i(s,y_i)}{\partial y_k}\right]_{y_j = y'_j} \qquad (A.1.4)$$

and j^0_{mk} and J^1_{mk} are the rectangular Jacobian matrices of order Nx2N for the gradients of the nonlinear boundary conditions:

$$J^0 = J^0_{mk} = \left[\frac{\partial g_m(y^0_j)}{\partial y^0_k}\right]_{y^0_j = y^{0,}_j} \qquad (A.1.5)$$

$$J^1 = J^1_{mk} = \left[\frac{\partial g_m(y^1_j)}{\partial y^1_k}\right]_{y^1_j = y^{1,}_j} \qquad (A.1.6)$$

Upon substitution of Equations A.1.3 and A.1.4 into Equation A.1.1 and A.1.2, the boundary-value problem can thus be written as:

$$\frac{dy_i}{ds} = a_{ik}(s)\, y_k + b_i(s) \qquad (A.1.7)$$

with boundary conditions

$$c^0_{mk}\, y^0_{mk} + d^0_m = 0 \qquad (A.1.8a)$$

$$c^1_{mk}\, y^1_{mk} + d^1_m = 0 \qquad \text{(A.1.8b)}$$

where $a_{ik} = J_{ik}$ (A.1.9a)

$$b_i = f_i(s,y_i) - J_{ik}\, y'_k \qquad \text{(A.1.9b)}$$

$$c^0_{mk} = J^0_{mk} \qquad \text{(A.1.9c)}$$

$$d^0_m = g_m(y^{0\prime}_j) - J^0_{mk}\, y^{0\prime}_k \qquad \text{(A.1.9d)}$$

$$c^1_{mk} = J^1_{mk} \qquad \text{(A.1.9e)}$$

$$d^1_m = h_m(y^1_j) - J^1_{mk}\, y^{1\prime}_k \qquad \text{(A.1.9f)}$$

Equation A.1.7 with boundary conditions A.1.8 and coefficients defined by A.1.9 constitutes a linear boundary value problem for an improved solution y_j in terms of functions for the previous trial h'_i. Further improved solutions are obtained by successive iteration in Equations A.1.5 to A.1.9 with y'_i, $y^{0\prime}$, and $y^{1\prime}$ replaced by the y_i, y^0_i, y^1_i generated by the previous iteration. The iteration process continues until the difference between y_i and y'_i is less than a stipulated accuracy.

A.2 DECOMPOSITION OF LINEAR BOUNDARY-VALUE PROBLEM

A linear two-point boundary-value problem such as that posed by Equations A.1.7 and A.1.8 can be solved by first decomposing the problem into a set of initial-value problems and then recombining solutions to each initial-value problem (Ref A-4, A-5, A-6). The advantage of using this method for solving a two-point boundary-value problem rather than a different method is that large sets of matrix equation coefficients need not be generated, stored in the computer memory, and solved simultaneously. Only a small number of coefficients at the starting and terminating points need to be considered. According to Ince (Ref A-7), the solution to each one of a linear set of 2N first-order differential equations can be considered as a linear combination of the solutions of N+1 initial-value problems, hereafter called partial solutions.

Assume the solutions to Equation A.1.7 can be written as:

$$y_i = z_i^0 + e_n z_i^n \qquad \text{(A.2.1)}$$

where e_n, n = 1,2,..., N are undetermined parameters and z_i^0 and z_i^n are partial solutions. The partial solution z_i^0 is the particular solution to:

$$\frac{dz_i^0}{ds} = a_{ik} z_k^0 + b_i \qquad \text{(A.2.2a)}$$

subject to actual "initial" conditions at s = 0

$$c0_{mk} z0_k^0 + d0_m = 0 \qquad \text{(A.2.2b)}$$

and fictitious "initial" conditions at s = 0

$$\mathbf{c0}_{mk} z0_k^0 + \mathbf{d0}_m^0 = 0 \qquad \text{(A.2.2c)}$$

The partial solutions z_i^n, n = 1,2,...,N are homogeneous solutions to

$$\frac{dz_i^n}{ds} = a_{ik} z_k^n \qquad n = 1,2,...,N \qquad \text{(A.2.3a)}$$

subject to actual "initial" conditions at s = 0

$$c0_{mk} z0_k^n = 0 \qquad n = 1,2,...,N \qquad \text{(A.2.3b)}$$

and fictitious "initial" conditions at s = 0

$$\mathbf{c0}_{mk} z0_k^n + \mathbf{d0}_m^n = 0 \qquad n = 1,2,...,N \qquad \text{(A.2.3c)}$$

The choice of fictitious initial conditions coefficients $\mathbf{c0}_{mk}$, $\mathbf{d0}_m^0$, $\mathbf{d0}_m^n$ is such that $\mathbf{d0}_m^n$ are linearly independent vectors and $\mathbf{c0}_{mk}$ is a rectangular Nx2N matrix of coefficients which allows an inverse of the assembled 2Nx2N square matrix C_{jk} of initial value coefficients:

$$C_{jk} = \left[\frac{C0_{mk}}{\mathbf{C0}_{mk}}\right] \qquad \begin{matrix} j,k = 1,2,...,2N \\ m = 1,2,...,N \end{matrix} \qquad \text{(A.2.4)}$$

to obtain solutions for $z0_k^0$ and $z0_k^n$ as:

$$z0_k^0 = - C_{jk}^{-1} \left[\frac{d0_m}{d0_m^0} \right] \tag{A.2.5}$$

$$z0_k^n = - C_{jk}^{-1} \left[\frac{0}{d0_m^n} \right] \tag{A.2.6}$$

The $d0_m^n$ are usually taken as Kronecker delta functions and $d0_m^n$ as a null vector.

Having defined N+1 linearly independent initial-value problems, each of which satisfies the actual boundary conditions at s = 0, one integrates each problem to the terminating point, s = 1. The partial solutions obtained at the terminating point are then used to determine the appropriate parameters, e_n, in Equation A.2.1 for the linear combination of partial solutions. The boundary conditions expressed by Equation A.1.8b at s = 1 can be written in terms of partial solutions as:

$$c1_{mk}(z1_k^0 + e_n\ z1_k^n) + d1_m = 0 \tag{A.2.7}$$

where $z1_k^0$ and $z1_k^n$ are the terminal values of the partial solutions. The product $c1_{mk}z1_k^n$ is a square NxN matrix and thus,

$$e_n = -\left[c1_{mk}\ z1_k^n\right]^{-1}\left(d1_m + c1_{mk}\ z1_k^0\right) \tag{A.2.8}$$

With e_n determined, a final initial-value integration of Equation A.1.7 can be performed with initial values:

$$y0_k = z0_k^0 + e_n\ z0_k^n \tag{A.2.9}$$

REFERENCES

A-1. B. Carnahan, H.A. Luther, and J.O. Wilkes. Applied numerical methods. Chichester, NY, John Wiley and Sons, 1969.

A-2. R. Bellman. "Functional equation in the theory of dynamic programming, V-positivity and quasi-linearity," in Proceedings of the National Academy of Sciences, vol 41, 1955.

A-3. R. Kalaba. "On nonlinear differential equations - The maximum operation and monotone convergence," Journal of Mathematical Mechanics, vol 8, 1959.

A-4. E.S. Lee. "Quasi-linearization, nonlinear boundary value problems and optimization," Chemical Engineering Science, vol 21, 1966.

A-5. A. Kalnins, and J.F. Lestingi. "On nonlinear analysis of elastic shells of revolution," Journal of Applied Mechanics, ASCE Transactions, vol 34, 1967, pp 59-64.

A-6. J.W. Leonard. "Dynamic response of initially-stressed membrane shells," Journal of the Engineering Mechanics Division, ASCE, vol 95(EM5), 1969, pp 1231-1253.

A-7. E.L. Ince. Ordinary differential equations. London, England, Longmans, Green and Co., 1927.

Appendix B

REDUCTION IN DIAMETER OF AN OPDS HOSE UNDER TENSION

The Navy Offshore Petrolem Discharge System (OPDS) relies on a 6-inch (inner diameter) rubber hose for fuel transfer. The hose is made of multilayer elastomeric material fortified with two-ply contra-helical wire reinforcements to withstand the external tension loads. The hose stretches to almost 45 percent of its original length at fracture (Figure 3 in main text). In the meantime, the outside diameter of the hose reduces 40 percent. This significant size reduction tends to shut down the fuel flow and totally disable the hoseline. Research for hose construction techniques to control the hose neck-down is currently underway, which will be addressed in the final project documentation of the Advanced Collapsible Pipe Program. This analysis is to examine the change in the inner diameter of the hose under tension. Elastomer is generally treated as an incompressible material. Its total volume does not change when subjected to external forces (Ref B-1). Referring to the definition sketch, Figure B-1, the total volume of the hose wall, V, can be expressed as:

$$V = \Pi D t \ell$$

in which $D = (D_o + D_i)/2$

where D_o = outer diameter
D_i = inner diameter
D = mean diameter
t = wall thickness of the hose
ℓ = total length of the hose

Since the elastomer is assumed incompressible,

$$\frac{\Delta V}{V} = \frac{\Delta D}{D} + \frac{\Delta t}{t} + \frac{\Delta \ell}{\ell} = 0 \qquad \text{(B-1)}$$

where Δ is the differential.

Replacing the mean diameter D with $D_o - t$ and assuming that $D_o >> t$:

$$D = D_o - t$$

$$= D_o \left(1 - \frac{t}{D_o}\right)$$

$$\frac{\Delta D}{D} = \frac{\Delta (D_o - t)}{D_o (1 - t/D_o)} = \left(1 + \frac{t}{D_o}\right) \left(\frac{\Delta D_o}{D_o} - \frac{\Delta t}{D_o}\right)$$

Substitution $\Delta D/D$ into Equation B-1 and neglecting the second order term $\Delta t/D_o$,

$$\frac{\Delta t}{t} = - \left[\frac{\Delta \ell}{\ell} + (1 + \frac{t}{D_o}) \frac{\Delta Do}{D_o} \right] \qquad \text{(B-2)}$$

Therefore, the variation of the wall thickness under tension can be expressed in terms of the elongation and the outer diameter reduction of the hose. Table B-1 summarizes the results of Equation B-2 using the empirical data shown in Figure 3 in the main text. The far right column shows that the variation in the wall thickness is less than 6 percent, even though the outer diameter of the hose reduces more than 40 percent. This result implies that a substantial reduction occurs in the inner diameter.

REFERENCE

B-1. E.P. Popov. Introduction to mechanics of solids, Englewood Cliffs, NJ, Prentice-Hall, 1968.

Table B-1. The Diameter reduction of the Navy Hose Under Tension.

Tension (kips)	O.D. (in)	$d\ell/\ell$	dD_o/D_o	$1+t/D_o$	dt/t
0.0	7.8	-	-	-	-
10.0	6.9	0.0734	-0.0548	1.1176	-0.0122
20.0	6.1	0.0940	-0.1159	1.1229	0.0262
30.0	5.6	0.0469	-0.0820	1.1441	0.0469
40.0	5.3	0.0261	-0.0536	1.1643	0.0363
50.0	5.0	0.0109	-0.0566	1.1799	0.0559
60.0	4.9	0.0144	-0.0200	1.2013	0.0096
70.0	4.8	0.0106	-0.0204	1.2074	0.0140
80.0	4.7	0.0070	-0.0208	1.2147	0.0183
90.0	4.7	0.0174	0.0000	1.2233	-0.0174

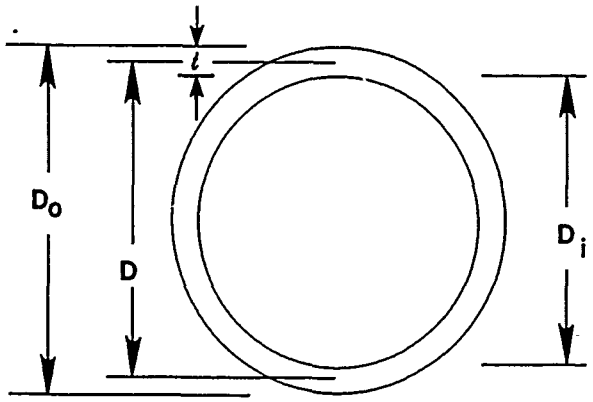

Figure B-1. Definition sketch of a cross section.

DISTRIBUTION LIST

ARMY LOGC ALC/ATCI-MS (Morrissett), Fort Lee, VA
ADMINSUPU PWO, Bahrain
CBC Code 10, Davisville, RI; Code 15, Port Hueneme, CA; Code 155, Port Hueneme, CA; Library, Davisville, RI; PWO (Code 400), Gulfport, MS; Tech Library, Gulfport, MS
CG FMF Pac, SCIAD (G5) Camp HM Smith, HI
CINCLANTFLT CE Supp Plans Offr, Norfolk, VA
CINCPACFLT Code 442, Pearl Harbor, HI
CNA Tech Library, Alexandria, VA
CNO DCNO, Logs, OP-424C, Washington, DC; DCNO, Logs, OP-452, Washington, DC
COMCBLANT Code S3T, Norfolk, VA
COMFAIR Med, SCE, Naples, Italy
COMFLEACT PWO, Kadena, Japan
COMNAVAIRSYSCOM Code 41712A, Washington, DC; Code 422, Washington, DC
COMNAVBEACHGRU ONE, CO, San Diego, CA
COMNAVLOGPAC Code 4318, Pearl Harbor, HI
COMNAVMARIANAS Code N4, Guam
COMNAVRESFOR Code 08, New Orleans, LA
COMNAVSUPPFORANTARCTICA DET, PWO, Christchurch, NZ
COMNAVSURF Code N42A, Norfolk, VA; Lant, CO, Norfolk, VA; Pac, Code N-4, San Diego, CA
COMSURFWARDEVGRU CO, Norfolk, VA
COMUSNAV CENT, Code N42, Pearl Harbor, HI
COMOPTEVFOR CO, Norfolk, VA
DEPCOMOPTEVFORPAC Code 705, San Diego, CA
DTIC Alexandria, VA
DTRCEN Code 125, Annapolis, MD; Code 1250, Annapolis, MD; Code 2842, Annapolis, MD; Code 4111, Bethesda, MD; Code 4120, Annapolis, MD
MAG 16, CO, MCAS Tustin, CA
MARCORBASE PAC, PWO, Camp Butler, JA; PWO, Camp Pendleton, CA; Pac, FE, Camp Butler, JA
MARCORDIST 12, Code 4, San Francisco, CA
MARCORPS FIRST FSSG, Engr Supp Offr, Camp Pendleton, CA
MARINE CORPS HQ LFL, Washington, DC; LMA-2/ME (Ferris), Washington, DC
MCAS Code 6EDD, Iwakuni, Japan
MCRDAC M & L Div Quantico, VA; NSAP Rep, Quantico, VA
NAF PWO, Atsugi, Japan
NAS Chase Fld, Code 18300, Beeville, TX; Code 072E, Willow Grove, PA; Code 163, Keflavik, Iceland; Code 18E, Bermuda; Code 83, Patuxent River, MD; PWO (Code 182) Bermuda; PWO, Adak, AK; PWO, Glenview, IL; PWO, Keflavik, Iceland; PWO, Sigonella, Italy; PWO, South Weymouth, MA; PWO, Willow Grove, PA; SCE, Barbers Point, HI; SCE, Norfolk, VA; Whidbey Is, PW-2, Oak Harbor, WA; Whiting Fld, PWO, Milton, FL
NAVAIRDEVCEN Code 832, Warminster, PA
NAVAIRENGCEN PWO, Lakehurst, NJ
NAVAIRTESTCEN PWO, Patuxent River, MD
NAVAVNDEPOT Code 61000, Cherry Point, NC
NAVCHAPGRU Code 30, Williamsburg, VA
NAVCOASTSYSCEN CO, Panama City, FL; Code 2360, Panama City, FL; Tech Library, Panama City, FL
NAVCOMMSTA Code 401, Nea Makri, Greece; PWO, Exmouth, Australia
NAVCONSTRACEN CO, Port Hueneme, CA; Code D2A, Port Hueneme, CA
NAVELEXCEN DET, OIC, Winter Harbor, ME
NAVFAC Centerville Bch, PWO, Ferndale, CA; PWO, Oak Harbor, WA
NAVFACENGCOM Code 00, Alexandria, VA; Code 03, Alexandria, VA; Code 03T (Essoglou), Alexandria, VA; Code 04A, Alexandria, VA; Code 04A3C, Alexandria, VA; Code 04A4E, Alexandria, VA; Code 04B3, Alexandria, VA; Code 0631, Alexandria, VA; Code 07, Alexandria, VA; Code 09M124 (Lib), Alexandria, VA; Code 163, Alexandria, VA
NAVFACENGCOM - CHES DIV. FPO-1PL, Washington, DC
NAVFACENGCOM - LANT DIV. Br Ofc, Dir, Naples, Italy; Code 1112, Norfolk, VA; Code 403, Norfolk, VA; Code 405, Norfolk, VA; Library, Norfolk, VA
NAVFACENGCOM - NORTH DIV. Code 04AL, Philadelphia, PA; Code 11, Philadelphia, PA; Code 202.2, Philadelphia, PA; Code 408AF, Philadelphia, PA
NAVFACENGCOM - PAC DIV. Code 09P, Pearl Harbor, HI; Code 2011, Pearl Harbor, HI; Library, Pearl Harbor, HI
NAVFACENGCOM - SOUTH DIV. Code 406, Charleston, SC; Library, Charleston, SC
NAVFACENGCOM - WEST DIV. 09P/20, San Bruno, CA; Code 04A2.2 (Lib), San Bruno, CA; Code 04B, San Bruno, CA; Code 408.2 (Jeung) San Bruno, CA; Pac NW Br Offc, Code C/50, Silverdale, WA

NAVFACENGCOM CONTRACTS OICC NW, Code 114NW, Silverdale, WA; OICC, Guam; OICC/ROICC, Norfolk, VA; ROICC (Code 495), Portsmouth, VA; ROICC, Corpus Christi, TX; ROICC, Keflavik, Iceland; ROICC, Point Mugu, CA; ROICC, Twentynine Palms, CA; SW Pac, OICC, Manila, RP; Trident, OICC, St Marys, GA
NAVHOSP SCE, Pensacola, FL; SCE, Yokosuka, Japan
NAVMARCORESCEN LTJG Davis, Raleigh, NC
NAVMEDCOM SCE, Jacksonville, FL
NAVOCEANSYSCEN Code 94, San Diego, CA
NAVPETOFF Code 40, Alexandria, VA; Code 8D107, Alexandria, VA
NAVPETRES Director, Washington DC
NAVPHIBASE PWO, Norfolk, VA
NAVSCSCOL PWO, Athens, GA
NAVSHIPYD Norfolk, Code 411, Portsmouth, VA
NAVSTA CO, Long Beach, CA; Engrg Dir, PWD, Rota, Spain; PWO, Mayport, FL; WC 93, Guantanamo Bay, Cuba
NAVSUPPO Sec Offr, La Maddalena, Italy
NAVSWC Code E211 (Miller), Dahlgren, VA; Code G-52 (Duncan), Dahlgren, VA; Code W42 (GD Haga), Dahlgren, VA
NAVWARCOL Code 24, Newport, RI
NAVWPNCEN AROICC, China Lake, CA; Code 2637, China Lake, CA
NAVWPNSTA Code 093, Yorktown, VA; Earle, PWO (Code 09B), Colts Neck, NJ; PWO, Yorktown, VA
NAVWPNSUPPCEN PWO, Crane, IN
NETC PWO, Newport, RI
NCR 20, CO; 20, Code R70
NMCB 3, Ops Offr; 40, CO; 5, Ops Dept; 74, CO
NRL Code 6123 (Dr Brady), Washington, DC
NSC Cheatham Annex, PWO, Williamsburg, VA; Code 44, Oakland, CA; Code 54.1, Norfolk, VA; Code 700, Norfolk, VA; SCE, Charleston, SC
PHIBCB 1, CO, San Diego, CA; 1, ELCAS Offcr, San Diego, Ca; 1, P&E, San Diego, CA; 2, CO, Norfolk, VA
PWC Code 10, Great Lakes, IL; Code 10, Oakland, CA; Code 101 (Library), Oakland, CA; Code 102, Oakland, CA; Code 123-C, San Diego, CA; Code 30, Norfolk, VA; Code 30V, Norfolk, VA; Code 400, Pearl Harbor, HI; Code 420, Great Lakes, IL; Code 424, Norfolk, VA; Code 505A, Oakland, CA; Code 614, San Diego, CA; Code 700, Great Lakes, IL; Library (Code 134), Pearl Harbor, HI; Library, Guam, Mariana Islands; Library, Norfolk, VA; Library, Pensacola, FL; Library, Yokosuka, Japan; Tech Library, Subic Bay, RP
SEAL TEAM 6, Norfolk, VA
SPCC PWO (Code 08X), Mechanicsburg, PA
CORRIGAN, LCDR S. USN, CEC, Stanford, CA

NCEL DOCUMENT EVALUATION

You are number one with us; how do we rate with you?

We at NCEL want to provide you our customer the best possible reports but we need your help. Therefore, I ask you to please take the time from your busy schedule to fill out this questionnaire. Your response will assist us in providing the best reports possible for our users. I wish to thank you in advance for your assistance. I assure you that the information you provide will help us to be more responsive to your future needs.

R. N. STORER, Ph.D, P.E.
Technical Director

DOCUMENT NO. _____ TITLE OF DOCUMENT: _____

_____

Date: _____ Respondent Organization : _____

Name: _____ Activity Code: _____
Phone: _____ Grade/Rank: _____

Category (*please check*):

Sponsor ____ User ____ Proponent ____ Other (*Specify*) _____

Please answer on your behalf only; not on your organization's. Please check (*use an X*) only the block that most closely describes your attitude or feeling toward that statement:

SA Strongly Agree A Agree O Neutral D Disagree SD Strongly Disagree

---

	SA	A	N	D	SD
1. The technical quality of the report is comparable to most of my other sources of technical information.	( )	( )	( )	( )	( )
2. The report will make significant improvements in the cost and or performance of my operation.	( )	( )	( )	( )	( )
3. The report acknowledges related work accomplished by others.	( )	( )	( )	( )	( )
4. The report is well formatted.	( )	( )	( )	( )	( )
5. The report is clearly written.	( )	( )	( )	( )	( )
6. The conclusions and recommendations are clear and directly supported by the contents of the report.	( )	( )	( )	( )	( )
7. The graphics, tables, and photographs are well done.	( )	( )	( )	( )	( )

Do you wish to continue getting NCEL reports? ☐ YES ☐ NO

Please add any comments (e.g., in what ways can we improve the quality of our reports?) on the back of this form.

Comments:

Please fold on line and staple

DEPARTMENT OF THE NAVY

Naval Civil Engineering Laboratory
Port Hueneme, CA 93043-5003

Official Business
Penalty for Private Use $300

Code L03B
NAVAL CIVIL ENGINEERING LABORATORY
PORT HUENEME, CA 93043-5003

INSTRUCTIONS

The Naval Civil Engineering Laboratory has revised its primary distribution lists. The bottom of the label on the reverse side has several numbers listed. These numbers correspond to numbers assigned to the list of Subject Categories. Numbers on the label corresponding to those on the list indicate the subject category and type of documents you are presently receiving. If you are satisfied, throw this card away (or file it for later reference).

If you want to change what you are presently receiving:

- Delete – mark off number on bottom of label.
- Add – circle number on list.
- Remove my name from all your lists – check box on list.
- Change my address – line out incorrect line and write in correction **(DO NOT REMOVE LABEL).**
- Number of copies should be entered after the title of the subject categories you select.

Fold on line below and drop in the mail.

Note: Numbers on label but not listed on questionnaire are for NCEL use only, please ignore them.

Fold on line and staple.

DEPARTMENT OF THE NAVY

Naval Civil Engineering Laboratory
Port Hueneme, CA 93043-5003

Official Business
Penalty for Private Use, $300

NO POSTAGE
NECESSARY
IF MAILED
IN THE
UNITED STATES

BUSINESS REPLY CARD

FIRST CLASS PERMIT NO. 12503 WASH D.C.

POSTAGE WILL BE PAID BY ADDRESSEE

Commanding Officer
Code L34
Naval Civil Engineering Laboratory
Port Hueneme, California 93043-5003

DISTRIBUTION QUESTIONNAIRE

The Naval Civil Engineering Laboratory is revising its Primary distribution lists.

SUBJECT CATEGORIES

1 SHORE FACILITIES
2 Construction methods and materials (including corrosion control, coatings)
3 Waterfront structures (maintenance/deterioration control)
4 Utilities (including power conditioning)
5 Explosives safety
6 Aviation Engineering Test Facilities
7 Fire prevention and control
8 Antenna technology
9 Structural analysis and design (including numerical and computer techniques)
10 Protective construction (including hardened shelters, shock and vibration studies)
11 Soil/rock mechanics
14 Airfields and pavements

15 ADVANCED BASE AND AMPHIBIOUS FACILITIES
16 Base facilities (including shelters, power generation, water supplies)
17 Expedient roads/airfields/bridges
18 Amphibious operations (including breakwaters, wave forces)
19 Over-the-Beach operations (including containerization, material transfer, lighterage and cranes)
20 POL storage, transfer and distribution

28 ENERGY/POWER GENERATION
29 Thermal conservation (thermal engineering of buildings, HVAC systems, energy loss measurement, power generation)
30 Controls and electrical conservation (electrical systems, energy monitoring and control systems)
31 Fuel flexibility (liquid fuels, coal utilization, energy from solid waste)
32 Alternate energy source (geothermal power, photovoltaic power systems, solar systems, wind systems, energy storage systems)
33 Site data and systems integration (energy resource data, energy consumption data, integrating energy systems)
34 ENVIRONMENTAL PROTECTION
35 Hazardous waste minimization
36 Restoration of installations (hazardous waste)
37 Waste water management and sanitary engineering
38 Oil pollution removal and recovery
39 Air pollution

44 OCEAN ENGINEERING
45 Seafloor soils and foundations
46 Seafloor construction systems and operations (including diver and manipulator tools)
47 Undersea structures and materials
48 Anchors and moorings
49 Undersea power systems, electromechanical cables, and connectors
50 Pressure vessel facilities
51 Physical environment (including site surveying)
52 Ocean-based concrete structures
54 Undersea cable dynamics

TYPES OF DOCUMENTS

85 Techdata Sheets 86 Technical Reports and Technical Notes
83 Table of Contents & Index to TDS
82 NCEL Guides & Abstracts
91 Physical Security

☐ None-remove my name